JOURNAL OF COMPUTATIONAL PHYSICS 106, 176–198 (1993)

Construction of TVD-like Artificial Viscosities on Two-Dimensional Arbitrary FEM Grids

PAUL ARMINJON

Université de Montréal, Département de Mathématiques et de Statistique, C.P. 6128 Succursale A, Montreal, Quebec, Canada H3C 3J7

AND

ALAIN DERVIEUX

INRIA, Sophia-Antipolis, 2004 Route des Lucioles, 06560 Valbonne, France

Received January 3, 1991

Quasi-second-order accurate oscillation-free schemes for the Euler equations are constructed by adjunction of an artificial viscosity term, with a coefficient determined according to symmetric TVD theory, to a two-step FEM/finite volume Richtmyer–Galerkin scheme on arbitrary (unstructured) FEM grids. Numerical experiments involving transonic and supersonic compressible flows are presented.

CONTENTS

1. INTRODUCTION

1.1. *Outline*

We consider the numerical resolution of nonlinear hyperbolic systems of conservation laws in one space dimension

$$U_t + F(U)_x = 0 \tag{1.1}$$

or in several space dimensions

$$U_t + \sum_{i=1}^{d} F_i(U)_{x_i} = 0, \tag{1.2}$$

where $U = (u_1, ..., u_m)^T$ and $F(U)$, $F_i(U)$ are m-component column vectors depending on time t and one or several coordinates x or $x_1, ..., x_d$.

System (1.1) can also be written as a quasi-linear system

$$U_t + A(U)\, U_x = 0, \tag{1.1'}$$

where $A = \partial F/\partial U$, with a similar form $U_t + \sum_{i=1}^{d} A_i(U)\, U_{x_i} = 0$ for (1.2).

First-order *upwind* schemes, derived from Steger and Warming's extension via flux splitting [51] of the Courant–Isaacson–Rees [62] scheme to nonlinear hyperbolic systems, usually lead to exceedingly *viscous* (*dissipative*) schemes, which tend to "smear" nonstationary shocks and other discontinuities. The introduction by Lax and Wendroff [26], followed by MacCormack [63] of *second-order centered schemes* was accompanied, despite a substantial improvement in the overall accuracy, by the problem of

0021-9991/93 $5.00

damping or eliminating the *oscillations* which appear in the neighborhood of discontinuities. This was done, originally, by introducing in the scheme an additional "*artificial viscosity*" term [35] which required a problem-dependent treatment, admittedly a rather awkward prerequisite for engineering applications.

Another approach consists in introducing a change of monotonicity "detector" [9, 27] which can find the nodes, where monotonicity is broken, and then trigger an efficient countermeasure, in the form of a flux limiter or slope limiter ([9, 27, 28, 10] to name only a few contributions).

More recently, the concept of TVD (total variation diminishing) schemes introduced by Harten [21, 71], extending ideas on monotonicity which had been proposed, for linear schemes, by Godunov [18], has led to a wide range of first and higher order accurate methods, which proved to be extremely useful both theoretically and in real engineering applications.

In this paper, we shall present a method for two- and three-dimensional problems, which uses a Richtmyer two-step scheme for numerical integration with respect to time and triangular (tetrahedral) finite elements for spatial discretization, while applying several recent symmetric TVD scheme essential features as described in the one-dimensional case by Davis [11] and Jameson [60],[1] and adapted to finite element formulations.

Before introducing our method, we shall examine in some detail, in the remainder of this section, some of the most important methods which have been designed to eliminate the oscillations of the Lax–Wendroff or MacCormack schemes, with the emphasis on upwind TVD schemes.

In Section 2 we describe Davis' symmetric (non-upwind) scheme, after a short review of Sweby's general formulation of flux-limited second-order accurate upwind TVD schemes, in the one-dimensional linear scalar case. Section 3 presents the extension to nonlinear hyperbolic systems.

In Section 4, we introduce the first-order conservative upwind FEM scheme of Baba–Tabata [8] for a scalar conservation equation and extend it to two- or three-dimensional systems.

Section 5 gives a short description of the P_1-Galerkin scheme, introduces a "finite volume Galerkin" version, and presents the two-step Richtmyer–Galerkin scheme which will serve as a basis for the construction of our oscillation-free schemes.

In Section 6 we give some indications on how to re-instate positivity or the maximum principle property by introducing some artificial viscosity in the scheme. Section 7 presents the three schemes proposed in this paper and describes some numerical results.

[1] We recently found out that the notion presented in Davis' scheme was also contained in a paper by Jameson, with a slightly different presentation.

1.2. *The Flux-Corrected Transport Algorithm of Boris and Book*

In their flux-corrected transport algorithm (FCT), Boris and Book designed a two-stage conservative scheme which strictly preserves mass and the positivity of the density ρ. The first stage, which is conservative and diffusive, can be written, in the particular case $\rho_t + v\rho_x = 0$ (with constant velocity v) of the one-dimensional continuity equation $\rho_t + (\rho v)_x = 0$, as

$$\rho_j^{n+1} = \rho_j^n - \frac{\nu}{2}(\rho_{j+1}^n - \rho_{j-1}^n) + \left(\frac{\nu^2}{2} + \frac{1}{8}\right)(\rho_{j+1}^n - 2\rho_j^n + \rho_{j-1}^n), \tag{1.3}$$

where $\nu \equiv v\,\Delta t/\Delta x$ which is the classical Lax–Wendroff scheme modified by a strong diffusion term $\frac{1}{8}(\rho_{j+1}^n - 2\rho_j^n + \rho_{j-1}^n)$.

The second stage tries to counterbalance this excessive diffusion; normally, one would expect that adding an equal amount of negative viscosity according to the scheme

$$\rho_j^{n+1} \to \bar{\rho}_j^{n+1} = \rho_j^{n+1} - (f_{j+1/2} - f_{j-1/2}) \quad \text{with} \quad f_{j+1/2} \equiv \tfrac{1}{8}(\rho_{j+1}^{n+1} - \rho_j^{n+1}) \tag{1.4}$$

would remove the numerical errors introduced in stage I, but it turns out that this also may lead to negative values of the density ρ and generate new maxima or minima, or accentuate already existing extrema, in contradiction with the monotonicity properties of the convection equation. Boris and Book's ingenious remedy was to introduce "*corrected*" values of the antidiffusive mass flux $f_{j+1/2}$ in (1.4), obtained by insisting that "no transfer of mass due to the antidiffusive flux should carry the density at any grid-point beyond the values at the two neighbouring points." This condition was satisfied by using in (1.4), instead of $f_{j+1/2}$, the *corrected flux*

$$f_{j+1/2}^c = \operatorname{sgn}\Delta_{j+1/2}\max\{0; \min(\Delta_{j-1/2}\operatorname{sgn}\Delta_{j+1/2}; \tfrac{1}{8}|\Delta_{j+1/2}|; \Delta_{j+3/2}\operatorname{sgn}\Delta_{j+1/2})\}, \tag{1.5}$$

where

$$\Delta_{j+1/2} \equiv \Delta\rho_{j+1/2} \equiv \rho_{j+1}^{n+1} - \rho_j^{n+1},$$

and $\frac{1}{8}$ is an adhoc coefficient, close to $\frac{1}{8}$, defined in [9].

The FCT strategy and its modified "phoenical FCT" version [64] for transport/convection equations, generally bring appreciable accuracy improvements in regions of

rapid variation or shocks. Intuitively, they can interpreted as

I. Applying a substantial amount of diffusion everywhere, in order to maintain stability and positivity.

II. Recovering the therewith lost accuracy by applying the negative of the diffusion used in I, everywhere except near extremas of ρ, where oscillations might occur and where one therefore tries to keep some or all of the diffusive effect of I, the appropriate amount of antidiffusion effectively applied being determined by the action of the flux correction (1.5).

In Parrot and Christie [41], Loehner *et al.* [33], and Selmin [65] two-dimensional methods based on finite element spatial discretizations and the flux-corrected transport algorithm are presented.

1.3. *van Leer's Monotonic Upstream-Centered Conservative Schemes*

(a) *van Leer's monotonic version of Fromm's second-order upwind conservative scheme.* Following a different approach, van Leer [66, 27] first observed that the Lax–Wendroff scheme can be made *monotonic* if one gives up the conservation form; to obtain a *second-order accurate monotonic scheme in conservation form*, he showed that Fromm's scheme for the convection equation $u_t + au_x = 0$ with $a > 0$ and $\sigma \equiv a\,\Delta t/\Delta x$:

$$u_j^{n+1} = u_j^n - \sigma(u_j^n - u_{j-1}^n) - \frac{\sigma}{4}(1-\sigma) \times [(u_{j+1}^n - u_j^n) - (u_{j-1}^n - u_{j-2}^n)] \tag{1.7}$$

or in van Leer's notation (see (1.12b) below)

$$\Delta_F^t u_j^n = -\sigma \Delta_{-1/2} u_j^n - \frac{\sigma}{4}(1-\sigma)(\Delta_{1/2} u_j^n - \Delta_{-3/2} u_j^n) \tag{1.7'}$$

can be regarded as the average of the Lax–Wendroff and Beam–Warming schemes:

$$\Delta_{\mathrm{LW}}^t u_j^n = -\sigma \Delta_{-1/2} u_j^n - \frac{\sigma}{2}(1-\sigma)(\Delta_{1/2} u_j^n - \Delta_{-1/2} u_j^n) \tag{1.8}$$

$$\Delta_{\mathrm{BW}}^t u_j^n = -\sigma \Delta_{-1/2} u_j^n - \frac{\sigma}{2}(1-\sigma)(\Delta_{-1/2} u_j^n - \Delta_{-3/2} u_j^n). \tag{1.9}$$

Each of these is now made *monotonic* by adding a nonlinear feedback corrective term of the form

$$\frac{\sigma}{2}(1-\sigma)\, Q(\theta_j)(\Delta_{1/2} u_j^n - \Delta_{-1/2} u_j^n) \tag{1.10}$$

to the Lax–Wendroff scheme and

$$\frac{\sigma}{2}(1-\sigma)\, R(\theta_{j-1})(\Delta_{-1/2} u_j^n - \Delta_{-3/2} u_j^n) \tag{1.11}$$

to the Beam–Warming scheme, respectively; the parameter θ_j is van Leer's *smoothness monitor*

$$\theta_j = \frac{\Delta_{j+1/2} u_j^n}{\Delta_{j-1/2} u_j^n} \tag{1.12a}$$

and van Leer's notation reads

$$\begin{aligned} &\Delta^t u_j^n \equiv u_j^{n+1} - u_j^n; \\ &\Delta_{1/2} u_j^n \equiv \Delta_+ u_j^n = u_{j+1}^n - u_j^n \\ &\Delta_{-3/2} u_j^n \equiv \Delta_{j-3/2} u^n = u_{j-1}^n - u_{j-2}^n \equiv \Delta_- u_{j-1}^n. \end{aligned} \tag{1.12b}$$

Although each "corrected" scheme, while being monotonic, is no longer in conservation form, van Leer succeeded in bringing the averaged scheme in conservation form,

$$\begin{aligned} \Delta_{\mathrm{FM}}^t u_j^n = &-\sigma \Delta_{-1/2} u_j^n \\ &-\frac{\sigma}{4}(1-\sigma)(\Delta_{1/2} u_j^n - \Delta_{-3/2} u_j^n) \\ &+\frac{\sigma}{4}(1-\sigma)\{S(\theta_j)(\Delta_{1/2} u_j^n - \Delta_{-1/2} u_j^n) \\ &- S(\theta_{j-1})(\Delta_{-1/2} u_j^n - \Delta_{-3/2} u_j^n)\} \end{aligned} \tag{1.13}$$

by taking

$$Q(\theta_j) = S(\theta_j) \qquad \text{and} \qquad R(\theta_{j-1}) = -S(\theta_{j-1}) \tag{1.14}$$

with

$$S(\theta_j) = \frac{|\theta_j| - 1}{|\theta_j| + 1} \text{ for any value of } \theta_j. \tag{1.15}$$

The subscript FM in (1.13) stands for "Fromm monotonic."

van Leer's scheme, which was successfully tested on a variety of numerical applications, represents an essential contribution to the solution of the problems caused by the oscillations appearing in the neighborhood of shock waves in gas dynamical computations.

(b) *van Leer's monotonic higher order upwind Godunov-type schemes.* Another contribution made by van Leer [28]

consists, in an attempt to improve on Godunov's first-order conservative method, in approximating the initial distribution by simple basic functions, e.g., piecewise Legendre polynomials of order one or higher, rather than by piecewise constant functions, then convecting explicitly the approximate distribution, and finally remapping the resulting distribution on each mesh in terms of the basic functions.

Different kinds of respresentations of the initial distribution in terms of the basic functions lead to second- and third-order schemes, and several monotonicity-preserving strategies, using slope limiters, lead to van Leer's oscillation-free upstream-centered higher order Godunov-type "MUSCL" schemes, another important contribution to the subject; see also [30, 59].

1.4. *Harten's Total Variation Diminishing schemes*

In a more analytical way, Harten [21, 71] laid the foundations of the theory of total variation diminishing (TVD) schemes, which rests on the monotonicity properties of weak solutions of the scalar conservation equation

$$u_t + f(u)_x \equiv u_t + a(u)\, u_x = 0. \tag{1.16}$$

For any such solution (see [25]) we have the following properties:

M1. No new local maximum or minimum can appear for $t > 0$

M2. The value of a local maximum is nonincreasing, that of a local minimum is nondecreasing; and therefore

M3. The total variation $\mathrm{TV}[u(t)] \equiv \sup \sum_j |u(x_{j+1}, t) - u(x_j, t)|$ is a nonincreasing function of time t.

Considering an explicit scheme *in conservation form* for (1.16),

$$\begin{aligned} u_j^{n+1} &= u_j^n - \lambda(h_{j+1/2} - h_{j-1/2}) \\ &\equiv H(u_{j-l}^n, u_{j-l+1}^n, \ldots, u_{j+m}^n)(\lambda \equiv \Delta t/\Delta x), \end{aligned} \tag{1.17}$$

where the "*numerical flux*" $h_{j+1/2} = h(u_{j-l+1}, \ldots, u_j, \ldots, u_{j+m})$ satisfies the "*consistency*" condition

$$h(v, v, \ldots, v) = f(v) \text{ (value of the original flux function)}, \tag{1.18}$$

Harten shows that

(i) a *monotone* scheme, for which H is a monotone nondecreasing function of each of its $(l+m+1)$ arguments, is necessarily *total variation diminishing* (TVD):

$$\sum_{j=-\infty}^{\infty} |u_j^{n+1} - u_{j-1}^{n+1}| \leqslant \sum_{j=-\infty}^{\infty} |u_j^n - u_{j-1}^n| \tag{1.19}$$

and

(ii) a TVD scheme is *monotonicity preserving*; i.e.,

$$\text{if } \{u_j^n\} \text{ is a monotone mesh function, so is } \{u_j^{n+1}\}. \tag{1.19'}$$

Using the mean value theorem, one can write scheme (1.17) in Harten's form

$$u_j^{n+1} = u_j^n - C_{j-1/2}\, \Delta u_{j-1/2}^n + D_{j+1/2}\, \Delta u_{j+1/2}^n \tag{1.20}$$

and prove *Harten's lemma* [21].

LEMMA. *If*

$$C_{j-1/2} \geqslant 0,\ D_{j+1/2} \geqslant 0, \text{ and } 0 \leqslant C_{j+1/2} + D_{j+1/2} \leqslant 1 \tag{1.21}$$

then scheme (1.20) *is TVD.*

In [21], Harten considers a three-point Q-scheme, in the form (1.17) with

$$h_{j+1/2} = \tfrac{1}{2}[f_j + f_{j+1} - Q(a_{j+1/2})\, \Delta u_{j+1/2}], \tag{1.22}$$

where Q, the coefficient of numerical viscosity, is an appropriate function of λ and $a_{j+1/2}$ with

$$a_{j+1/2} \equiv \begin{cases} \Delta f_{j+1/2}/\Delta u_{j+1/2} & \text{if } \Delta u_{j+1/2} \neq 0 \\ (df/du)_j \equiv a(u_j) & \text{if } \Delta u_{j+1/2} = 0. \end{cases} \tag{1.23}$$

By truncation error analysis (see [67, 21]) one can show that

(i) the (generally) first-order TVD scheme (1.17)–(1.22) leads to a *second-order* approximation to the modified equation

$$u_t + f(u)_x = \Delta x(\sigma(a)\, u_x)_x \tag{1.24}$$

with

$$\sigma(a) = \frac{1}{2} Q(a) - \frac{\lambda}{2} a^2 \tag{1.25}$$

and

(ii) applying the Q-scheme to the modified equation

$$u_t + (f+g)_x = 0 \tag{1.26}$$

with

$$g(u) \equiv \Delta x(\sigma(a)\, u_x) \tag{1.26'}$$

gives a second-order approximation of the original inviscid equation (1.16).

To ensure that the additional flux function g be differentiable, the effective numerical flux $h_{j+1/2}$ for (1.26) is obtained with a smoothing procedure [68] that leads to Harten's explicit five-point, second-order accurate TVD schemes. These schemes, which can be written in conservation form, can also be extended to implicit TVD second-order schemes [58, 71] and to hyperbolic systems of conservation laws; they are endowed with most of the properties desirable for applications to compressible flow problems: high accuracy, monotonicity preservation, stability in the total variation norm. They are well suited to compute steady-state solutions [71, p. 18; 58], and they can be tuned to be consistent with an entropy inequality; this implies convergence of the scheme to the unique weak solution satisfying the entropy condition, which is the only physically relevant solution.

More recently, the idea of symmetric TVD schemes was introduced independently by Davis [11] and Jameson [60, 70] and elaborated on by Yee [69]. Essentially, it consists in adding an artificial viscosity term to a Lax–Wendroff scheme and making sure that the corresponding scheme satisfies Harten's TVD criterion. In [11] Davis first added an upstream-centered artificial viscosity, but then removed the upwind character of the scheme by means of symmetrization, thus obtaining a slightly more viscous TVD scheme at nearly no cost in the effective accuracy. We shall examine Davis' scheme in the next section.

2. SYMMETRIC TVD SCHEMES: THE ONE-DIMENSIONAL SCALAR LINEAR CASE

For the scalar linear convection equation

$$u_t + au_x = 0,\ a = \text{const} > 0 \tag{2.1}$$

the specific advantages of symmetric (Lax–Wendroff) or upwind (Beam–Warming) second-order accurate schemes for the construction of TVD schemes have been studied, among others, by Roe [47], Chakravarthy and Osher [39], Sweby [52], Jameson [70, 60], Davis [11], Yee [69].

Sweby gave an elegant construction of a second-order accurate upwind scheme which is made TVD by the action of a flux limiter; Sweby's scheme, which unifies some of the most efficient flux-limited schemes (Roe, Osher, van Leer), starts from the Lax–Wendroff scheme, conveniently rewritten in the form

$$u_j^{n+1} = u_j^n - \nu\, \Delta_{-1/2} u_j^n - \Delta_- \left[\frac{\nu(1-\nu)}{2} \Delta_{1/2} u_j^n \right]. \tag{2.2}$$

As we must have $0 \leqslant \nu \leqslant 1$ for stability, the second-order difference can be viewed as an anti-diffusive term, superposed to the diffusive effect of the first difference term (the CIR scheme term). Wherever u is smooth, this second-order correction is desirable, but it should be reduced in the vicinity of discontinuities if we want to avoid oscillations. Following [9, 27], Sweby therefore introduces a "flux limiter" $\phi(r_j)$ as a multiplicative factor in the antidiffusive flux, depending in a nonlinear way on the smoothness sensor

$$r_j = \frac{\Delta_{-1/2} u_j^n}{\Delta_{1/2} u_j^n} \equiv \frac{u_j^n - u_{j-1}^n}{u_{j+1}^n - u_j^n} \equiv r_j^+, \tag{2.3}$$

thus leading to the *flux-limited Lax–Wendroff scheme* $(a > 0)$

$$u_j^{n+1} = u_j^n - \nu\, \Delta_{-1/2} u_j^n - \tfrac{1}{2}\nu(1-\nu)\, \Delta_- [\phi(r_j)\, \Delta_{1/2} u_j^n]. \tag{2.4}$$

For negative characteristic velocity $(a < 0)$, we have, similarly,

$$u_j^{n+1} = u_j^n - \nu\, \Delta_{1/2} u_j^n + \tfrac{1}{2}\nu(1+\nu)\, \Delta_- [\phi(r_{j+1}^-)\, \Delta_{1/2} u_j^n], \tag{2.4'}$$

where

$$r_j^- \equiv \frac{\Delta_{1/2} u_j^n}{\Delta_{-1/2} u_j^n} = \frac{u_{j+1}^n - u_j^n}{u_j^n - u_{j-1}^n}. \tag{2.3'}$$

As r_j will be negative at or near an extremum, one sets $\phi(r_j) = 0$ for $r_j \leqslant 0$ to inhibit the generation of oscillations.

The flux-limiter function $\phi(r)$ is thus seen to control the net amount of upwinding included in the scheme: for $0 < \phi(r) \ll 1$, Sweby's scheme resembles the CIR scheme with which it coincides for $r \leqslant 0$, as one takes $\phi(r) = 0$ for $r \leqslant 0$ [52]; for $\phi(r) = 1$, it is identically the LW scheme; for $\phi(r) = r$, we obtain the Beam–Warming scheme. For a second-order accurate TVD scheme, the graph of $\phi(r)$ must be located in the hatched area shown in Fig. 1.

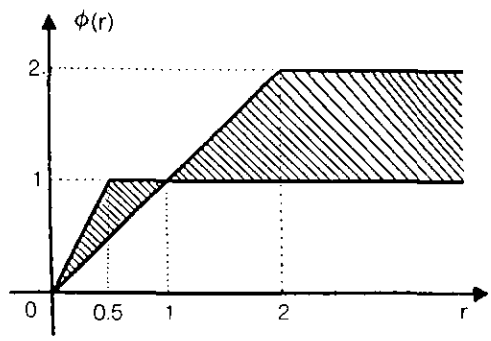

FIG. 1. Second-order TVD region, Sweby's scheme.

Important examples of such flux limiter functions are

(a) van Leer's limiter

$$\phi_{vL}(r)=\begin{cases}\dfrac{2r}{1+r} & r\geqslant 0\\ 0 & r\leqslant 0.\end{cases} \tag{2.5}$$

(b) Chakravarthy and Osher's limiter

$$\phi_{CO}(r)=\max[0,\min(r,\Phi)] \text{ for some parameter } \Phi,\quad 1\leqslant\Phi\leqslant 2. \tag{2.6}$$

(c) Roe's "*superbee*" limiter

$$\begin{aligned}&\phi(r)=0 && \text{if} \quad r\leqslant 0,\\ &\phi(r)=2r && \text{if} \quad 0\leqslant r\leqslant \tfrac{1}{2},\\ &\phi(r)=1 && \text{if} \quad \tfrac{1}{2}\leqslant r\leqslant 1,\\ &\phi(r)=r && \text{if} \quad 1\leqslant r\leqslant 2,\\ &\phi(r)=2 && \text{for} \quad r\geqslant 2.\end{aligned} \tag{2.7}$$

This is the most compressive (anti-diffusive) limiter.

(d) Roe's "*minmod*" limiter (the least compressive or the most diffusive limiter)

$$\phi(r)=\begin{cases}\min(r,1), & r\geqslant 0\\ 0, & r\leqslant 0.\end{cases} \tag{2.8}$$

(e) Davis' limiter

$$\begin{aligned}&\phi(r)=\min(2r,1), && \text{if} \quad 0\leqslant r<\infty,\\ &\phi(r)=0 && \text{if} \quad r\leqslant 0.\end{aligned} \tag{2.9}$$

(f) Palmerio's parabolic limiter (private communication, 1986)

$$\begin{aligned}&\phi(r)=r(2-r) && \text{if} \quad 0\leqslant r<1,\\ &\phi(r)=1 && \text{if} \quad r\geqslant 1\end{aligned} \tag{2.9'}$$

which has the advantage of being a smooth function of r while being nearly as compressive as Davis' limiter for $0\leqslant r\leqslant 1$.

We shall now briefly describe *Davis' scheme*. Considering first $u_t+au_x=0$ with $a>0$ (constant) and adding an upstream-centered artificial viscosity

$$K^+_{j+1/2}(r^+_j)\,\Delta u_{j+1/2}-K^+_{j-1/2}(r^+_{j-1})\,\Delta u_{j-1/2} \quad \text{with} \quad r^+_j=\Delta u_{j-1/2}/\Delta u_{j+1/2} \tag{2.10}$$

to the Lax–Wendroff scheme (2.2) gives, after factorizing $\Delta u_{j-1/2}\equiv u^n_j-u^n_{j-1}$ to enhance the case of positive velocity in Harten's form,

$$u^{n+1}_j=u^n_j-C_{j-1/2}\,\Delta u_{j-1/2}+D_{j+1/2}\,\Delta u_{j+1/2} \tag{2.11}$$

with

$$C_{j-1/2}=\nu\left[1+\frac{1}{2}(1-\nu)\left(\frac{1}{r^+_j}-1\right)\right]-\left(\frac{K^+_{j+1/2}}{r^+_j}-K^+_{j-1/2}\right),\qquad D_{j+1/2}\equiv 0 \tag{2.12}$$

which coincides with Sweby's scheme (2.4) if we take

$$K^+_{j+1/2}=\tfrac{1}{2}\nu(1-\nu)[1-\phi(r^+_j)], \tag{2.13}$$

thus obtaining Davis' form of an upwind diffusively corrected Lax–Wendroff scheme

$$\begin{aligned}u^{n+1}_j&=u^n_j-\nu\,\Delta u_{j-1/2}\\ &\quad-\Delta_-\left[\frac{\nu}{2}(1-\nu)\,\Delta u_{j+1/2}\right]\\ &\quad+\Delta_-(K^+_{j+1/2}\,\Delta u_{j+1/2})\\ &=u_j-\nu\Delta_-\,[u_j+\tfrac{1}{2}(1-\nu)\,\Delta u_{j+1/2}]\\ &\quad+\Delta_-(K^+_{j+1/2}\,\Delta u_{j+1/2}).\end{aligned} \tag{2.14}$$

(For simplicity, we write $\Delta u_{j+1/2}$ for $\Delta u^n_{j+1/2}\equiv\Delta_- u^n_{j+1}=\Delta_+ u^n_j\equiv u^n_{j+1}-u^n_j$.)

For $0\leqslant\phi<1$ and $0\leqslant\nu\leqslant 1$, the last term is easily seen to be *of diffusive character*, and due to the action of the flux limiter in the viscosity coefficient (2.13), Davis' scheme appears as an interpolate between a second-order centered scheme (LW) and a second-order centered scheme augmented with a uniform artificial viscosity (this latter scheme being first-order accurate), as opposed to the representation of Sweby's scheme (2.4) as a hybrid scheme between a first-order upwind and a second-order centered scheme; the blending is controlled by the flux limiter, through the coefficient $1-\phi(r^+_j)$ appearing in $K_{j+1/2}$.

Considering now the case $a<0$, Davis' scheme takes the form

$$u^{n+1}_j=u^n_j-\nu\,\Delta u_{j+1/2}+\Delta_-\,[\tfrac{1}{2}\nu(1+\nu)\,\Delta u_{j+1/2}]+\Delta_-(K^-_{j+1/2}\,\Delta u_{j+1/2}) \tag{2.15}$$

which coincides with Sweby's scheme if we choose

$$K^-_{j+1/2}=\tfrac{1}{2}\nu(1+\nu)[\phi(r^-_{j+1})-1]. \tag{2.16}$$

Combining the cases $a>0$, $a<0$ and defining new coefficients of artificial viscosity

$$K^+_{j+1/2}=\begin{cases}\frac{1}{2}\nu(1-\nu)[1-\phi(r^+_j)] & \text{if } a>0\\ 0 & \text{if } a\leqslant 0\end{cases} \tag{2.17a}$$

$$K^-_{j+1/2}=\begin{cases}0 & \text{if } a>0\\ \frac{1}{2}\nu(1+\nu)[\phi(r^-_{j+1})-1] & \text{if } a<0\end{cases} \tag{2.17b}$$

and adding, according to the flux-splitting principle [51], both artificial viscosity terms appearing in (2.14)–(2.15), with their built-in upwinding, to the Lax–Wendroff scheme in its original form, we obtain Davis' form of a Lax–Wendroff scheme with an *upstream-centered artificial viscosity*

$$\begin{aligned}u^{n+1}_j=u^n_j&-\frac{\nu}{2}(u^n_{j+1}-u^n_{j-1})\\&+\frac{\nu^2}{2}(u^n_{j+1}-2u^n_j+u^n_{j-1})\\&+\Delta_-[\{K^+_{j+1/2}(r^+_j)+K^-_{j+1/2}(r^-_{j+1})\}\,\Delta u_{j+1/2}].\end{aligned} \tag{2.18}$$

To eliminate the requirement of determining which direction is upwind and therewith obtain a *symmetric quasi-second-order accurate TVD scheme*, Davis redefines the artificial viscosity coefficients in (2.18) as

$$\begin{aligned}K^+_{j+1/2}&=\tfrac{1}{2}|\nu|\,(1-|\nu|)[1-\phi(r^+_j)]\\K^-_{j+1/2}&=\tfrac{1}{2}|\nu|\,(1-|\nu|)[1-\phi(r^-_{j+1})].\end{aligned} \tag{2.19}$$

These coefficients which no longer depend on the upwind direction, lead to a slightly larger artificial viscosity, in the neighbourhood of shocks, but very roughly the same dissipation as in Sweby's scheme, away from discontinuities.

In the examples presented by Davis [11], no noticeable spreading of the shocks can be observed, while some benefic "smoothing" effect of the augmented (symmetric) artificial viscosity can be observed in the case of Burgers' equation (the "kink" in the rarefaction is nearly completely eliminated in Fig. 3 of [11], see also [4]).

In some computations associated with the present work, instead of taking the sum of both artificial viscosity terms contributed by leftward and rightward waves, as indicated in Davis' formulation (2.18)–(2.19), we shall take their *maximum*

$$K_{j+1/2}=\max(K^+_{j+1/2},K^-_{j+1/2}), \tag{2.20}$$

thus obtaining an artificial viscosity which lies between Sweby's and Davis' viscosities.

Before presenting the extension of Davis' scheme to hyperbolic systems, let us first mention that to apply it to nonlinear scalar equations (1.16), $u_t+f(u)_x=u_t+a(u)\,u_x=0$, it suffices to consider the *local characteristic speed* $a_{j+1/2}$ defined in (1.23).

3. SYMMETRIC TVD SCHEMES FOR HYPERBOLIC SYSTEMS

3.1. *Scalar Viscosity*

Let us consider first the linear system

$$U_t+AU_x=0, \tag{3.1}$$

where $U=(u_1,\ldots,u_m)$ is an m-vector and $A=(A_{ij})$ a constant $m\times m$ matrix.

Assuming that (3.1) is hyperbolic means that the eigenvalues a_i of A are real and that there exists a complete set of linearly independent right eigenvectors, forming a matrix P such that

$$P^{-1}AP=\wedge=\begin{pmatrix}a_1 & & & 0\\ & a_2 & & \\ & & \ddots & \\ 0 & & & a_m\end{pmatrix}. \tag{3.2}$$

Letting $V=P^{-1}U$ and multiplying (3.1) by P^{-1} gives

$$P^{-1}U_t+P^{-1}AU_x=V_t+P^{-1}APV_x=V_t+\wedge V_x=0 \tag{3.3}$$

which is a system of uncoupled scalar equations, each of which can now be solved using Davis' upwind scheme (2.18)–(2.17); after multiplying by P to return to the original dependent variables U, we obtain

$$\begin{aligned}U^{n+1}_j=U^n_j&-\frac{A\lambda}{2}(U^n_{j+1}-U^n_{j-1})\\&+\frac{A^2\lambda^2}{2}(U^n_{j+1}-2U^n_j+U^n_{j-1})\\&+\Delta_-\{P[K^+_{j+1/2}(r^+_j)\\&+K^-_{j+1/2}(r^-_{j+1})]\,P^{-1}(U^n_{j+1}-U^n_j)\},\end{aligned} \tag{3.4}$$

where

$$K^+_{j+1/2}=\operatorname{diag}(K^+_{i,j+1/2}),$$

$$K^+_{i,j+1/2}=\begin{cases}0 & \text{if } a_i\leqslant 0,\ i=1,\ldots,m\\ \frac{\nu_i}{2}(1-\nu_i)[1-\phi(r^+_{i,j})], & \text{else}\end{cases} \tag{3.5}$$

is the *artificial viscosity coefficient* (2.17) for the ith equa-

tion of (3.3), $v_i = a_i\lambda$, and $\lambda = \Delta t/\Delta x$; $r^+_{i,j} = (u_{i,j} - u_{i,j-1})/(u_{i,j+1} - u_{i,j})$.

Note. We would take, similarly,

$$K^-_{j+1/2} = \mathrm{diag}(K^-_{i,j+1/2}),$$

where

$$K^-_{i,j+1/2} = \begin{cases} \dfrac{v_i(1+v_i)}{2}\,[\phi(r^-_{i,j+1}) - 1], & \text{if } a_i \leqslant 0 \\ 0, & \text{if } a_i \geqslant 0. \end{cases}$$

Davis [11] proposed to remove the requirement to compute the matrices P, P^{-1} by approximating the diagonal matrices $K^{\pm}_{j+1/2}$ by *scalar matrices*, letting

$$K^{\pm}_{j+1/2}(r^{\pm}_j) = k^{\pm}_{j+1/2}(r^{\pm}_j) I, \tag{3.6}$$

where the artificial viscosity coefficients $k^{\pm}_{j+1/2}(r^{\pm}_j)$ are scalar functions of the scalar sensor $r^{\pm}_j$ defined by

$$r^+_j = \frac{(\Delta U^n_{j-1/2}, \Delta U^n_{j+1/2})}{(\Delta U^n_{j+1/2}, \Delta U_{j+1/2})} \tag{3.7a}$$

$$r^-_j = \frac{(\Delta U^n_{j-1/2}, \Delta U^n_{j+1/2})}{(\Delta U^n_{j-1/2}, \Delta U_{j-1/2})}. \tag{3.7b}$$

Davis also eliminates the *requirement to determine the upwind direction* by taking

$$k^{\pm}_{j+1/2}(r^{\pm}_j) = \tfrac{1}{2}C(v)[1 - \phi(r^{\pm}_j)], \tag{3.8}$$

where the CFL-number v is defined by

$$v = \lambda \max_{1 \leqslant i \leqslant m} |a_i| \tag{3.9}$$

and

$$C(v) = \begin{cases} v(1-v) & \text{if } v \leqslant 0.5 \\ \tfrac{1}{4} & \text{if } v > 0.5. \end{cases} \tag{3.10}$$

Since $0 \leqslant v(1-v) \leqslant \frac{1}{4}$ for $0 \leqslant v \leqslant 1$, this choice corresponds to taking the largest possible coefficient $v(1-v)$ in the definition of the symmetric artificial viscosity coefficient (2.19).

With these simplications, P and K commute and P, P^{-1} disappear from Davis' scheme (3.4), which takes the following *symmetric (nonupwind) form*

$$\begin{aligned} U^{n+1}_j = U^n_j &- \frac{\lambda}{2} A(U^n_{j+1} - U^n_{j-1}) \\ &+ \frac{\lambda^2}{2} A^2(U^n_{j+1} - 2U^n_j + U^n_{j-1}) \Delta_-[(K^+_{j+1/2}(r^+_j) \\ &+ K^-_{j+1/2}(r^-_{j+1})\}(U^n_{j+1} - U^n_j)], \end{aligned} \tag{3.11}$$

where $K^{\pm}_{j+1/2}$ and $r^{\pm}_j$ are defined by (3.6)–(3.8), and (3.7), respectively.

As this scheme no longer depends on the diagonalization $A \to P^{-1}AP = \Lambda$, it can be used without any modification for nonlinear systems.

In Davis' scheme (3.11), the artificial viscosity coefficient $k^{\pm}(r^{\pm}) = \frac{1}{2}C(v)[1 - \phi(r^{\pm}_j)] = \frac{1}{2}v(1-v)(1-\phi(r^{\pm}))$, for $0 \leqslant v \leqslant \frac{1}{2}$, may become insufficient in the case of two-dimensional problems solved with a finite element spatial discretization and a two-step Richtmyer-type time solver.

We shall choose instead, in this paper, the larger value

$$k^{\pm}_{j+1/2}(r^{\pm}_j) = \frac{\max |v_i|}{2}(1 - \phi(r^{\pm}_j)) \tag{3.12}$$

in order to compensate for the fact that, in two space dimensions with an FEM solver, the Galerkin formulation of the Laplacian term does not always lead to the desired monotonicity properties. In particular, this term no longer has the viscous effect observed for one-dimensional problems; indeed the matrix corresponding to Δu is not diagonally dominant (an M-matrix) if there are obtuse angles.

An advantage of our choice (3.12) is that we recover the viscosity of a first-order upwind scheme, whenever $1 - \phi(r) \cong 1$ (the CIR-scheme can indeed be written $u^{n+1}_j = u^n_j - (v/2)(u^n_{j+1} - u^n_{j-1}) + (|v|/2)(u^n_{j+1} - 2u^n_j + u^n_{j-1})$, thus providing for an easier achievement of monotonicity.

On the other hand, the main drawback lies in the reduced stability domain (just in the same manner as, say, for the diffusion equation $u_t = \nu u_{xx}$, the usual Euler scheme, forward in time and centered in space, is stable for $\nu\,\Delta t/(\Delta x)^2 \leqslant \frac{1}{2}$: the larger ν, the most restrictive this condition is on Δt).

3.2. *Scalar Sensor*

Another feature of this paper is concerned with our choice of the sensor or smoothness monitor r_j given by (3.7) in Davis' method.

We try to choose for r_j, instead of using U, a scalar dependent variable associated with the flow, such as the Mach number M or density ρ, which might be more appropriate to control the shock structure for this variable. The sensor's own monotonicity is thus directly controlled, rather than being buried in a scalar product as is the case with Davis' choice.

3.3. *Non-scalar sensor*

In the two-dimensional case, for example, we might use each of the primitive variables ρ, u, v, p as its own sensor in order to extrapolate it from t^n to t^{n+1}.

If a monotonicity test shows that, say, ρ has an extremum (or a discontinuity) the accuracy of the scheme is not

automatically *globally* reduced to first order, but only the extrapolations in time associated with ρ: using, for instance, van Leer's MUSCL algorithm, one then sets the corresponding slopes, in the piecewise linear representation of ρ, equal to zero; the scheme remains second-order accurate for the other dependent variables.

TVD schemes similar to the MUSCL algorithm and based on this strategy will therefore be less dissipative than a symmetric, Davis-type TVD scheme based on the choice (3.7) for the sensor, or on arbitrarily choosing one of the flow variables as sensor, and using the corresponding information to compute the flux limiter for all the flow variables. In this last case, we might suffer a drastic loss of accuracy if, for instance, we had chosen the density ρ as our sensor and tried to capture a contact discontinuity: the sensor would then command a total cancellation of the antidiffusion for *all* dependent variables, therewith globally reducing the accuracy to first order for all variables, while p, u, v are in fact continuous through the contact discontinuity and should be treated with some antidiffusion for second-order accuracy!

Another approach consists, rather than individually choosing ρ, u, v, p as their own sensors, in first diagonalizing the jacobian matrices $A = \partial F/\partial U$, $B = \partial G/\partial U$ (cf. (4.8)), by introducing the characteristic variables $V = T^{-1}U$ (see Section 4.4) and then taking each of these characteristic variables as its own sensor (cf. [69]).

4. FIRST-ORDER NON-OSCILLATORY TWO-DIMENSIONAL FEM SCHEMES

4.1. *Introduction*

One of the problems encountered when solving system (1.1) with finite element spatial discretizations consists in the inclusion of an appropriate amount of viscosity in order to ensure that a Lax–Wendroff-type time discretization becomes a Lax–Wendroff-type scheme, augmented with an artificial viscosity term, and enjoying appropriate monotonicity properties. This has been achieved by Donea [12] and Loehner *et al.* [33].

In the present work we try to obtain quasi-second-order accurate nearly monotonic two-dimensional schemes by following the approach used, in the construction of upwind first-order FEM schemes, by Baba and Tabata [8] who were able to prove some properties closely related to monotonicity (discrete maximum principle, positivity). Second-order time accuracy, away from extrema or stagnation points, will be provided by the use of a two-step Richtmyer–Galerkin scheme.

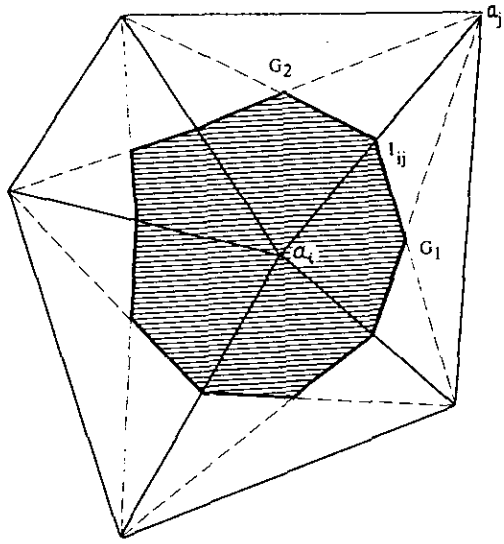

FIG. 2. Barycentric cell around a_i.

4.2. *The Baba–Tabata Conservative First-Order Upwind Scheme (Two-Dimensional Scalar Equation)*

Considering the simplified scalar equation

$$u_t + \operatorname{div}(\mathbf{V}u) = 0 \qquad \text{for} \quad (x, y) \in \Omega \quad \text{(bounded domain in } \mathbb{R}^2) \tag{4.1}$$

and using a finite volume formulation on the barycentric cells C_i constructed around the vertices a_i of the triangles of a regular finite element triangulation of Ω (Fig. 2; G_1, G_2 are centroids, I is a midpoint; see [8, 1] and Section 4.4), leads, upon integrating in the ith barycentric cell, to

$$\int_{C_i} u_t \, dx\, dy = -\int_{C_i} \operatorname{div}(\mathbf{V}u) \, dx\, dy = -\int_{\partial C_i} \mathbf{V}u \cdot \mathbf{n} \, d\sigma. \tag{4.2}$$

Using an explicit Euler first-order accurate time discretization gives (see Fig. 2, where $\Gamma_{ij} = \partial C_i \cap \partial C_j$ and C_j is the barycentric cell constructed around a node a_j adjacent to a_i)

$$\int_{C_i} \frac{u_i^{n+1} - u_i^n}{\Delta t} \, dx\, dy - \sum_{\substack{j \\ a_j \text{ adjacent to } a_i}} u_{\text{upwind}}(i, j) \int_{\Gamma_{ij}} \mathbf{V} \cdot \mathbf{n} \, d\sigma, \tag{4.3}$$

where

$$u_{\text{upwind}}(i, j) \equiv \begin{cases} u_i & \text{if } \int_{\Gamma_{ij}} \mathbf{V} \cdot \mathbf{n} \, d\sigma \geqslant 0 \\ u_j & \text{otherwise.} \end{cases} \tag{4.4}$$

This explicit scheme is *positive*, i.e., $u_i^n \geqslant 0$ for all $n > 0$ if

$u_0(x, y) \geqslant 0$, provided that the following sufficient condition holds [8, 3]):

$$\max \|\mathbf{V}\| \, \Delta t \, \text{length}(\partial C_i) \leqslant \text{area}(C_i) \tag{4.5}$$

for each barycentric cell C_i associated with the triangulation of Ω (this is obviously a condition of the CFL type). It also satisfies the maximum principle if the divergence of $\mathbf{V}$ is equal to zero.

4.3. *Enhancement of the Artificial Viscosity Included in the Baba–Tabata Scheme*

The Baba–Tabata scheme (4.3), (4.4) can be written as the sum of a centered scheme and a viscous term: if u_i^n denotes the numerical approximation of u at time t^n in the ith barycentric cell C_i, (4.3) can be written as

$$\int_{C_i} (u_i^{n+1} - u_i^n)\, dx\, dy + \Delta t \sum_{j \text{ neighbour of } i} \frac{u_i^n + u_j^n}{2} \int_{\Gamma_{ij}} \mathbf{V} \cdot \mathbf{n}\, d\sigma = \sum_{j \text{ neighbour of } i} M_{ij}(u_j^n - u_i^n)$$

$$\text{for} \quad i = 1, 2, \ldots, N_p, \tag{4.6}$$

where the summation is extended to the indices of the cells C_j which are adjacent to C_i, $\Gamma_{ij} = C_i \cap C_j$, N_p is the number of nodes in the FEM triangulation $\mathcal{T}_h$, and

$$M_{ij} = \frac{\Delta t}{2} \left| \int_{\Gamma_{ij}} \mathbf{V} \cdot \mathbf{n}\, d\sigma \right|. \tag{4.7}$$

The second term, in the LHS of (4.6), corresponds to a centered scheme, while the RHS can be shown to be of diffusive character.

To give a heuristic verification of the *diffusive* nature of $\sum_j M_{ij}(u_j^n - u_i^n)$, let us consider the simplified case of Fig. 3 and factorize out M_{ij}, temporarily assumed to be constant:

$$\sum_{j=1}^{4} (u_j - u_i) = [(u_1 - 2u_i + u_3) + (u_2 - 2u_i + u_4)]$$

which obviously approximates $h^2\, \Delta u_i$ (we have assumed that the diagonals of the quadrilateral 1234 are parallel to the axes and meet at node i, their common midpoint; here the quadrilateral 1234 is a rhombus).

Since $|\int_{\Gamma_{ij}} \mathbf{V} \cdot \mathbf{n}\, d\sigma| > 0$ we have (upon averaging these terms) a positive factor multiplying $h^2\, \Delta u_i$, which clearly is of diffusive nature.

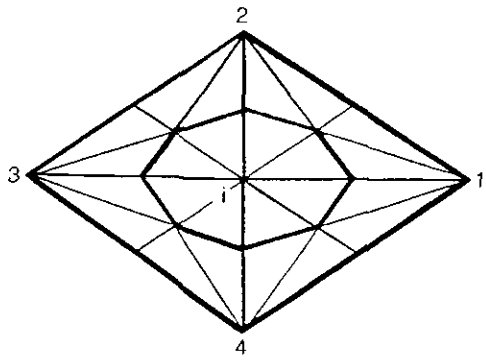

FIG. 3. A particular case.

4.4. *Extension of the Baba–Tabata Scheme to Two-Dimensional Systems*

The extension of these ideas to nonlinear hyperbolic systems of equations in two or three space dimensions has been done by Vijayasundaram [55–57]. For the two-dimensional system of conservation equations

$$U_t + F(U)_x + G(U)_y = 0 \tag{4.8}$$

an explicit, first-order accurate time discretization is

$$\frac{U^{n+1} - U^n}{\Delta t} + F(U^n)_x + G(U^n)_y = 0. \tag{4.9}$$

Let $\mathcal{T}_h$ be a triangulation of the computational domain $\Omega_h \subset \mathbb{R}^2$.

Let a_i be a node of $\mathcal{T}_h$ and T_{ij} $(1 \leqslant j \leqslant q_i)$ the triangles having a_i as a vertex with a numbering corresponding to counterclockwise rotation around a_i. Let a_{ij} $(1 \leqslant j \leqslant q_i)$ be the nodes adjacent to a_i; the line segment $a_i a_{ij}$ is the common side of T_{ij} and $T_{i,j+1}$, with the convention that $T_{i,q_i+1} = T_{i1}$. G_{ij} denotes the centroid of triangle T_{ij}, I_{ij} the middle point of $a_i a_{ij}$. The *integration zone* or *barycentric cell* C_i associated with node a_i is the region bounded by the line segments $G_{i1}I_{i1}$, $I_{i1}G_{i2}$, ..., $G_{iq_i}I_{iq_i}$, $I_{iq_i}G_{i1}$ (see Fig. 2 and 3, where the cell C_i is shaded).

Let V_h be the space of scalar piecewise constant functions, constant in each cell C_i. The approximation test function space W_h consists of piecewise constant d-dimensional vector functions constant on each cell. The approximation problem (to first-order accuracy) then consists in finding $U_h^{n+1} \in W_h = (V_h)^d$ (with $d = 3$, 4, or 5, depending on the number of space coordinates considered in the problem) such that

$$\int_{\Omega_h} \frac{U_h^{n+1} - U_h^n}{\Delta t} w_h\, dx\, dy + \int_{\Omega_h} \{F(U_h^n)_x + G(U_h^n)_y\}\, w_h\, dx\, dy = 0, \qquad \forall w_h \in (V_h)^d. \tag{4.10}$$

This equation holds if and only if it is satisfied coordinatewise for each scalar characteristic function $v_h = \chi_i$ associated with the cell C_i, since these form a basis for V_h; or iff it holds vectorwise for each $w_h = (\chi_i)^d \in (V_h)^d$. Equivalently, using the divergence theorem, U_h^{n+1} should satisfy

$$(U_i^{n+1} - U_i^n)\,\mathrm{Area}(C_i) + \Delta t \sum_{j=1}^{q_i} \int_{\Gamma_{ij}} \{F(U_h^n)\, v_x + G(U_h^n)\, v_y\}\, d\sigma = 0, \quad (4.11)$$

where $\Gamma_{ij} = \partial C_i \cap \partial C_{ij}$, C_{ij} being the adjacent cell centered at node a_{ij}.

Since the function U_h^n is discontinuous along the cell boundary element $\Gamma_{ij} = [G_{ij} I_{ij}; I_{ij} G_{i,j+1}]$ the flux functions $F(U_h^n)$ and $G(U_h^n)$ cannot be defined in a unique manner; they depend on their piecewise constant values in the cells C_i, C_{ij} on both sides of Γ_{ij}. Following [8, 56, 51, 1, 2], we introduce flux-splitting and upwinding in the computation of these flux functions. Defining (Fig. 4)

$$\begin{aligned} &\nu_{ij}^1 = (\nu_{xij}^1, \nu_{yij}^1) = \text{unit normal to } G_{ij} I_{ij}, \\ &\quad \text{pointing outward of } C_i \\ &\nu_{ij}^2 = (\nu_{xij}^2, \nu_{yij}^2) = \text{unit normal to } I_{ij} G_{i,j+1}, \\ &\quad \text{pointing outward of } C_i \\ &\eta_{xij} = \nu_{xij}^1\, \mathrm{length}(G_{ij} I_{ij}) + \nu_{xij}^2\, \mathrm{length}(I_{ij} G_{i,j+1}) \\ &\eta_{yij} = \nu_{yij}^1\, \mathrm{length}(G_{ij} I_{ij}) + \nu_{xij}^2\, \mathrm{length}(I_{ij} G_{i,j+1}), \end{aligned} \quad (4.12)$$

we can write system (4.11) as

$$(U_i^{n+1} - U_j^n)\,\mathrm{Area}(C_i) + \Delta t \sum_{j=1}^{q_i} H_{ij}^n = 0, \quad (4.13a)$$

where the values of the fluxes $F(U_h^n)$, $G(U_h^n)$ in the numerical boundary integral approximating (4.11),

$$H_{ij}^n = [\eta_{xij} F^n + \eta_{yij} G^n]_{\Gamma_{ij}}, \quad (4.13b)$$

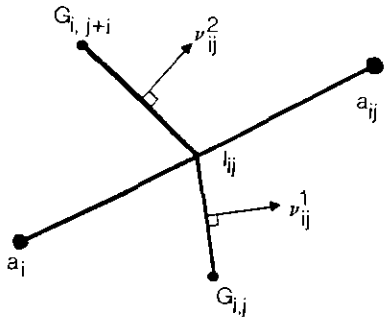

FIG. 4. Cell-boundary element Γ_{ij} associated with nodes a_i, a_{ij}.

will be determined with the help of flux-splitting and upwinding.

4.4.1. *Flux-splitting and upwinding.* The assumed hyperbolicity of system (4.8) means that for any $(\alpha_1, \alpha_2) \in \mathbb{R}^2$ and $U \in \mathbb{R}^d$, the eigenvalues of the matrix

$$M = \alpha_1 F'(U) + \alpha_2 G'(U) \quad (4.14)$$

are real, and the matrices M are uniformly diagonalizable; i.e., there exists, for each couple (α_1, α_2), a matrix $T_{\alpha_1\alpha_2}(U)$ such that

$$M = T_{\alpha_1\alpha_2}(U) \bigwedge_{\alpha_1\alpha_2} (U)\, T^{-1}_{\alpha_1\alpha_2}(U)$$
$$\text{or equivalently } T^{-1} M T = \bigwedge \quad (4.15)$$

where $\bigwedge = \bigwedge_{\alpha_1\alpha_2}(U)$ is a diagonal matrix having the same eigenvalues as M (see [51, pp. 280, 289]). Moreover, for the Euler equations the flux functions F, G are homogeneous of order one, i.e., $F(\lambda U) = \lambda F(U)$, so that

$$F(U) = F'(U) \cdot U, \qquad G(U) = G'(U) \cdot U. \quad (4.16)$$

With these properties, the numerical boundary integrals H_{ij}^n of Eq. (4.13) can be written

$$\begin{aligned} H_{ij}^n &= [\eta_{xij} F'(U_h^n) + \eta_{yij} G'(U_h^n)]\, U_h^n \\ &\equiv P_{ij}(U_h^n) \cdot U_h^n, \end{aligned} \quad (4.17a)$$

where P_{ij} can be factorized according to (4.15) and partitionned as in [51]:

$$\begin{aligned} P_{ij} &= T_{ij} \bigwedge_{ij} T_{ij}^{-1} = P_{ij}^+ + P_{ij}^- \\ &\equiv T_{ij} \bigwedge_{ij}^+ T_{ij}^{-1} + T_{ij} \bigwedge_{ij}^- T_{ij}^{-1}. \end{aligned} \quad (4.17b)$$

Introducing

$$P_{ij/2}^{\pm} = P_{ij}^{\pm}\left(\frac{U_i^n + U_{ij}^n}{2}\right) \quad (4.17c)$$

and following [55], we can choose the upwinding

$$H_{ij}^n = (P^+)_{ij/2}^n U_i^n + (P^-)_{ij/2}^n U_{ij}^n \quad (4.18)$$

in (4.13) and obtain an explicit, first-order accurate *flux-splitting upwind* FEM-FVM scheme for the two-dimensional Euler equations:

$$U_i^{n+1} = U_i^n - \frac{\Delta t}{\mathrm{Area}(C_i)} \left\{ \sum_{j=1}^{q_i} [(P^+)_{ij/2}^n U_i^n + (P^-)_{ij/2}^n U_{ij}^n] \right\}. \quad (4.19)$$

Note that scheme (4.19) can be written in Osher's semi-discrete form

$$\text{area}(\text{cell}_i)\frac{\partial U}{\partial t}+\sum_{j \text{ neighbour of } i}\Phi(U_i, U_j, \boldsymbol{\eta}_{ij})=0, \tag{4.20a}$$

where the nodes a_i, a_{ij} $(j=1, ..., q_i)$ have been relabelled i, j and j is simply one of the nodes adjacent to node i, and

$$\boldsymbol{\eta}_{ij}=\int_{\Gamma_{ij}}\mathbf{n}\,d\sigma\equiv\begin{pmatrix}\eta_{xij}\\ \eta_{yij}\end{pmatrix} \tag{4.20b}$$

with $\Gamma_{ij}\equiv\partial\,\text{cell}_i\cap\partial\,\text{cell}_j=G_1IG_2$ on Fig. 2.

In the sequel, we shall also consider schemes (4.20) for which the values of F, G in the boundary integral $\int_{\Gamma_{ij}}$ appearing in (4.11) are obtained with the help of an approximate Riemann solver, rather than with the above Baba–Tabata upwinding strategy.

We shall consider, in particular, Osher's approximate Riemann solver, written in the schematic form

$$\Phi(U_i, U_j, \boldsymbol{\eta}_{ij})=\tfrac{1}{2}\left[H(U_i)+H(U_j)-\int_{U_i}^{U_j}|P(U)|\,dU\right], \tag{4.21a}$$

where

$$\begin{aligned}H(U)&=\eta_{xij}F(U)+\eta_{yij}G(U),\\ P(U)&=\frac{\partial H(U)}{\partial U}\end{aligned} \tag{4.21b}$$

(see [40, 36, 39].

5. P_1-GALERKIN, FINITE-VOLUME GALERKIN, RICHTMYER–GALERKIN SCHEMES

5.1. *Finite Element/Finite Volume Galerkin Schemes*

Multiplying the scalar equation (4.1), $u_t+\text{div}(\mathbf{V}u)=0$, by a basis function ϕ_i associated, at node i, with a P_1-finite element triangulation $\mathcal{T}_h$ and integrating by parts leads to

$$(u_t, \phi_i)-(u\mathbf{V}, \text{grad}\,\phi_i)=0 \tag{5.1}$$

and thus to the P_1-*Galerkin scheme* for (4.1):

$$(u_t, \phi_i)-\sum_{j \text{ neighbour of } i}\text{area}(T_j)\cdot(u\mathbf{V})|_{T_j}\cdot(\text{grad}\,\phi_i)|_{T_j}=0, \tag{5.2}$$

where $(\cdot,\cdot)$ denotes the usual L^2-inner product, $(u\mathbf{V})|T_j$ is some average of $u\mathbf{V}$ on triangle T_j, and

$$\begin{aligned}(\text{grad}\,\phi_i)|_{T_j}&=\int_{T_j}\text{grad}\,\phi_i\,dx\,dy/\text{Area}(T_j)\\ &=\int_{I_1GI_2}\mathbf{n}\,d\sigma/\text{Area}\,T_j.\end{aligned} \tag{5.3}$$

As a preparation for subsequent use in the construction of non-oscillatory schemes and to establish a link between the Baba–Tabata scheme and the P_1-Galerkin scheme (5.2), it is convenient to introduce a variant of the latter scheme, the "*finite volume Galerkin*" formulation, obtained by integrating (4.1) on the barycentric cell centered at node i of $\mathcal{T}_h$, using Green's theorem and choosing a constant value $(u\mathbf{V})|_I$ for the function $u\mathbf{V}$ along the cell boundary element G_1IG_2,

$$\text{Area}(\text{cell}_i)\frac{\partial u_i}{\partial t}+\sum_{j \text{ neighbour of } i}(u\mathbf{V})|_I\cdot\int_{G_1IG_2}\mathbf{n}\,d\sigma=0, \tag{5.4}$$

where I is the midpoint of side ij and G_1, G_2 are the centroids of the two triangles sharing ij as a common side; the sum is taken over the vertices j which are endpoints of sides issuing from i. The relationship with the Baba–Tabata scheme rests on the following elementary property.

LEMMA 5.1. *The schemes* (5.2) *and* (5.4) *are* identical *if*

(i) *Mass matrix lumping by line summation is applied to* (5.2)

(ii) *The following numerical quadratures are applied*

— *for* (5.2),

$$(u\mathbf{V})|_T\cong\tfrac{1}{3}(u_i\mathbf{V}_i+u_j\mathbf{V}_j+u_k\mathbf{V}_k) \tag{5.5a}$$

where i, j, k are the vertices of triangle T

— *for* (5.4),

$$(u\mathbf{V})|_I\cong\tfrac{1}{2}(u_i\mathbf{V}_i+u_j\mathbf{V}_j). \tag{5.5b}$$

Introducing (ii) in (5.4), using Lemma 5.1, and choosing $\mathbf{V}=\text{const}$, on the other hand, in (4.6) written in the form

$$\begin{aligned}&\text{area}(\text{cell}_i)\frac{\partial u_i}{\partial t}+\sum_{j \text{ neighbour of } i}\left(\frac{u_i+u_j}{2}\right)\int_{G_1IG_2}\mathbf{V}\cdot\mathbf{n}\,d\sigma\\ &\quad=\tfrac{1}{2}\left[\sum_{j \text{ neighbour of } i}(u_j-u_i)\left|\int_{G_1IG_2}\mathbf{V}\cdot\mathbf{n}\,d\sigma\right|\right],\end{aligned} \tag{5.6}$$

we find that the Baba–Tabata scheme can be considered, in the case $\mathbf{V}=\text{constant}$, as a finite volume Galerkin/

P_1-Galerkin scheme augmented with an artificial (numerical) diffusion term (the right-hand side of (5.6)).

From this observation, we foresee two promising ways to construct quasi-second-order accurate oscillation-free schemes:

(i) Start from a Galerkin formulation and add some (TVD-theory controlled) artificial viscosity, second-order accuracy being aimed at by using a two-step Richtmyer-type time discretization to be described in the next subsection. This will be named the *Richtmyer–Galerkin–TVD–viscous approach* (Section 7.1).

(ii) Use the barycentric cell–finite volume approach combined with some upwinding. Here again, TVD-theory can be used to obtain an oscillation-free scheme. As the generalized Baba–Tabata approach is only first-order accurate, we must improve the accuracy, and one possible way to do so is to construct *a hybrid between a finite volume Galerkin scheme and an upwind scheme* (see Section 7.3).

5.2. *Richtmyer–Galerkin Schemes*

To solve a two-dimensional system of hyperbolic conservation equations

$$U_t + F(U)_x + G(U)_y = 0 + \text{boundary conditions} \quad (5.7)$$

(in our particular context (5.7) will represent the two-dimensional Euler equations for ideal compressible flow), where $U(x, y, t) = (u_k(x, y, t))$ is a vector in $\mathbb{R}^m$; we shall also use a two-step Richtmyer-type scheme based on a finite element spatial discretization [1–3].

We consider a triangulation $\mathcal{T}_h$ of a polygonal domain Ω_h which approximates the domain of interest Ω of the flow (h is a small positive parameter), and we introduce the spaces

$$\begin{aligned} H_h &= \{v \in L^2(\mathbb{R}^2);\ v \text{ is continuous;} \\ &\qquad v \text{ is linear on each triangle } T \in \mathcal{T}_h\} \\ K_h &= \{v \in L^2(\mathbb{R}^2); \\ &\qquad v \text{ is constant on each triangle } T \in \mathcal{T}_h\} \quad (5.8) \\ V_h &= H_h \cap H^1(\mathbb{R}^2) \\ S_h &= \{v \in L^2(\mathbb{R}^2); \\ &\qquad v|_{\text{cell}(i)} = \text{constant for each barycentric} \\ &\qquad \text{cell constructed at the nodes } i \text{ of } \mathcal{T}_h\} \end{aligned}$$

(see Section 4); i.e., $v \in S_h$ is piecewise constant, constant on each barycentric cell associated with $\mathcal{T}_h$.

Since the consistent mass matrix of the P_1-Galerkin discretization we would normally obtain is not diagonal, we introduce, to reduce computing costs, and following [54, 8, 23], a mass-lumping operator $\sum_0$ defined as the trivial projection from space V_h on to S_h:

$$\forall v \in V_h,\ \sum_0 v \in S \qquad \text{with} \quad \sum_0 v|_{\text{cell}\,i} = v(i) \qquad \text{for each node } i \text{ of } \mathcal{T}_h. \quad (5.9)$$

Then a natural adaptation of Richtmyer's method, in the context of finite element spatial discretizations, consists in considering a P_0-predictor step $U^n \to U^P = (U_k^P)_{k=1}^m$ (each component u_k^P of U^P is constant on each triangle $T \in \mathcal{T}_h$), using a control volume (resp. area) formulation, and a P_1-corrector step, somewhat simplified with the help of the mass-lumping operator $\sum_0$.

Lerat and Peyret [31] have shown that it may be profitable to introduce the length of the first time step as a parameter, writing the corresponding Richtmyer–Galerkin scheme as follows:

Step 1. *Predictor.* $U^n = (u_1^n, \ldots, u_m^n) \in (V_h)^m \to U^P \in (K_h)^m$ for each $T \in \mathcal{T}_h$ and $k = 1, \ldots, m$,

$$u_k^P(T) = \frac{1}{\text{area}(T)} \left\{ \iint_T u_k^n \, dx\, dy - \alpha\, \Delta t \int_{\partial T} [F_k(U^n) n_x + G_k(U^n) n_y] \, d\sigma \right\}. \quad (5.10a)$$

Step 2. *Corrector.* $U^P \to U^{n+1} \in (V_h)^m$: For each $\phi = (\phi_k) \in (V_h)^m$ and $k = 1, \ldots, m$,

$$\begin{aligned} &\iint_\Omega \sum_0 \left[\frac{u_k^{n+1} - u_k^n}{\Delta t} \right] \sum_0 \phi_k \, dx\, dy \\ &\quad = \iint_\Omega^* \left\{ \beta_1 \left[F_k(U^n) \frac{\partial \phi_k}{\partial x} + G_k(U^n) \frac{\partial \phi_k}{\partial y} \right] \right. \\ &\qquad \left. + \beta_2 \left[F_k(U^P) \frac{\partial \phi_k}{\partial x} + G_k(U^P) \frac{\partial \phi_k}{\partial y} \right] \right\} dx\, dy \\ &\qquad - \int_{\partial \Omega_h}^* \phi_k [F_k(U^n) n_x + G_k(U^n) n_y] \, d\sigma, \quad (5.10b) \end{aligned}$$

where $\beta_1 = (2\alpha - 1)/2\alpha$, $\beta_2 = 1/2\alpha$.

According to the one-dimensional study [31], we take for the optimal length of the first step

$$\alpha = 1 + \sqrt{5}/2$$

as numerical experiments have shown this choice to be advantageous, even for the computation of two-dimensional stationary shocks.

Numerical integration is necessary to compute the nonlinear terms (see the integrals indicated by *):

(a) a quadrature with lower accuracy is sufficient for the boundary integral in (5.10a), since it will be multiplied by $(\Delta t)^2$ in the resulting scheme

(b) a finer quadrature, exact for P_2-integrands, is needed for integrals with stars in the corrector (5.10b).

Note that:

(1) the last integral in (5.10b) (boundary fluxes) is not centered in time, for simplicity, and therefore only first-order accurate, although second-order accuracy is indeed preserved for steady-state computations. A more sophisticated variant using a boundary predictor and time centered boundary fluxes has also been tested, but brought no substantial improvements.

(2) For $\alpha = \frac{1}{2}$ (midpoint rule for the time integration, with the midpoint values given by the predictor), scheme (5.10) reduces essentially to the Taylor–Galerkin scheme introduced by J. Donea [12] and studied in [33].

6. STABILIZATION OF CENTERED SCHEMES

The (first- or second-order accurate) Galerkin, finite-volume Galerkin, and Richtmyer–Galerkin schemes introduced in Section 5 do not satisfy, in their conservation law formulation, the maximum principle or the conservation of positivity property which apply to Godunov's and other first-order monotone schemes.

To obtain these properties, it is necessary to introduce an appropriate viscous term in these schemes. Unfortunately, the spatial diffusion operators constructed with the Galerkin method seem to achieve this goal in a very unsatisfactory manner. In particular, the resulting matrices may cease to be M-matrices, as encountered, for example, in Baba–Tabata's scheme, as soon as obtuse angles appear in the triangulation; this may be a serious nuisance for three-dimensional calculations, as it is difficult to retriangulate to eliminate small/obtuse trihedral angles.

By contrast, viscosities of the form

$$\text{area}(\text{cell}_i)\, u_i \to \text{area}(\text{cell}_i)\, u_i + \sum_{j \text{ neighbour of } i} \alpha_{ij}(u_j - u_i) \qquad (6.1)$$

allow for an efficient reinforcement of positivity for the scheme, while maintaining its conservation form.

Here are, among others, two manners to obtain this type of viscosity:

(i) Method I ("MC-MD" method), using the difference between the mass matrices MC, MD. This method, which has been used in [33, 13], consists in introducing, for the viscosity operator, the difference between the P_1-Galerkin consistent mass matrix MC and the diagonalized (approximate) mass matrix MD.

A straightforward calculation shows that in two dimensions the viscosity coefficients α_{ij} are then given by

$$\alpha_{ij} = \frac{1}{12} \frac{\text{area}(T_{ij}^+) + (T_{ij}^-)}{\text{area}(\text{cell}_i)}, \qquad (6.2)$$

where T_{ij}^+, T_{ij}^- are the two triangles of $\mathcal{T}_h$ adjacent to side ij.

This approach does not take into account the length of the time step Δt and the velocity of the underlying waves and may therefore lead to schemes with rather unsophisticated viscosities such as, e.g., the Lax–Friedrichs scheme.

(ii) Method II (upwinding method). A convenient way to construct a more flexible viscosity consists in introducing the numerical viscosity generated by the upwinding of the Baba–Tabata method.

Here the viscosity coefficients are given by

$$\alpha_{ij} = \frac{\Delta t}{2} \left| \int_{\partial C_i \cap \partial C_j} \mathbf{V} \cdot \mathbf{n}\, d\sigma \right|. \qquad (6.3)$$

A careful study of these two viscosities (i)–(ii) leads to the following comments:

In the one-dimensional case, the "MC-MD" viscosity can be combined very efficiently with the Lax–Wendroff scheme to yield a monotonous method, the "MC-MD" viscosity adding itself in a natural way to the viscous effects of the Lax–Wendroff second-derivative term.

In the two-dimensional case, we somehow heuristically expect the "MC-MD" method to enjoy the same property; although we have not proved it, it seems to be fairly well verified by numerical tests.

On the other hand, the viscous term generated by upwinding is designed to match a first-order-centered derivative for monotonicity, and not a Lax–Wendroff-type second derivative.

7. QUASI-SECOND-ORDER ACCURATE SCHEMES

In this section we describe, as anticipated in the end of Section 5.1, oscillation-free finite element schemes which are nearly second-order accurate (i.e., second-order accurate away from shocks or other extremas).

7.1. *Richtmyer–Galerkin Scheme with Symmetric TVD Artificial Viscosity*

For the part of the computations described in this paper which has been performed with a Richtmyer–Galerkin scheme augmented with artificial viscosity, we have used a viscosity of type "MC-MD" (see (6.1)–(6.2)) to stabilize the scheme.

The *Richtmyer–Galerkin scheme* used here corresponds to the choice $\alpha = \frac{1}{2}$, $\beta_1 = 0$, $\beta_2 = 1$ in (5.10): using the equivalence mentioned in Lemma 5.1 between the P^1-Galerkin and the finite volume Galerkin formulations, we can reduce (5.10a) to the following (*coordinatewise*) form:

Predictor step. $U^n = (u_k^n) \in (V_h)^m \to U^P = (u_k^P) \in (K_h)^m$ such that

$$\begin{aligned} &\text{area}(T)(u_k^P)_T \\ &\quad = \int_T u_k^n \, dx\, dy - \frac{\Delta t}{2} \int_{\partial T} [F_k(U^n)\, n_x \\ &\qquad + G_k(U^n)\, n_y]\, d\sigma \end{aligned} \tag{7.1a}$$

for each triangle $T \in \mathcal{T}_h$ and $k = 1, \ldots, m$.

The corrector step (5.10b) can similarly be brought to the simplified form

Corrector step. $U^P \to U^{n+1} = (u_k^{n+1}) \in (V_h)^m$:

$$\begin{aligned} &\text{area}(\text{cell}_i)\{(u_k^{n+1})_i - (u_k^n)_i\} \\ &\quad = -\Delta t \sum_{T \text{ neighbour of } i} \int_{\partial\, \text{cell}_i \cap T} \\ &\qquad \times [F_k(U^P)\, n_x + G_k(U^P)\, n_y]\, d\sigma \\ &\qquad + \text{boundary fluxes.} \end{aligned} \tag{7.1b}$$

In the *Richtmyer–Galerkin TVD-viscous scheme*, we then add an artificial viscosity term with a TVD-controlled coefficient k_{ij} ("*artificial viscosity limiter*"); the proposed scheme can be written (*vectorwise*) as

$$\begin{aligned} &\text{area}(\text{cell}_i)(U_i^{n+1} - U_i^n) \\ &\quad = -\Delta t \left\{ \sum_{T \text{ neighbour of } i} \int_{\partial\, \text{cell}_i \cap T} [F(U^P)\, n_x + G(U^P)\, n_y] \right. \\ &\qquad \left. - \sum_{j \text{ neighbour of } i} k_{ij} \alpha_{ij} (U_j^n - U_i^n) \right\} + \text{boundary fluxes,} \end{aligned} \tag{7.1c}$$

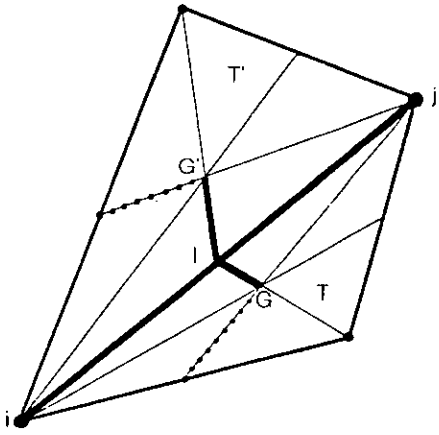

FIG. 5. Cell-boundary element $\Gamma_{ij} = \text{GIG}'$.

where α_{ij} is the viscosity coefficient defined in Section 6 with the help of MC-MD, $U_i^n = ((u_1^n)_i, \ldots, (u_m^n)_i)$ is the projection of the piecewise linear vector function $U^n \in (V_h)^m$ by $\sum_0$ on S_h, which is constant on cell_i (the barycentric cell centered at node i), and the artificial viscosity limiter k_{ij}, controlling the amount of viscosity added to the Richtmyer–Galerkin scheme, is defined as follows:

Construction of k_{ij}. Using the Mach number M as a sensor and following the one-dimensional approach defined by Davis, we need, for each cell-boundary element $\{GI, IG'\}$ (Fig. 5), four values of the sensor S at four points i, j, "$i-1$," "$j+1$" on the same line, the latter points being fictitious and such that the segments ["$i-1$", i], $[i, j]$, [j, "$j+1$"] have the same length (see Fig. 6).

To compute the fictitious values S_{i-1}^*, S_{j+1}^* at "$i-1$," "$j+1$," we introduce the *nodal gradients* grad $S(i)$, grad $S(j)$,

$$\text{grad } S(i) = \left(\iint \phi_i \, \text{grad } S \, dx\, dy \right) \Big/ \iint \phi_i \, dx\, dy, \tag{7.2}$$

where ϕ_i is the P_1-FEM basis function associated to node i, and using the nodal values $S(i)$, $S(j)$ we generate the *fictitious values*

$$\begin{aligned} S_{i-1}^* &= S(i) - 2\text{grad } S(i) \cdot \mathbf{ij} + [S(j) - S(i)] \\ S_{j+1}^* &= S(j) + 2\text{grad } S(j) \cdot \mathbf{ij} - [S(j) - S(i)]. \end{aligned} \tag{7.3}$$

From these four consecutive values we now compute Sweby's variation ratios, defined by (2.3),

$$r_{ij}^+ = \frac{S_i - S_{i-1}^*}{S_j - S_i}, \qquad r_{ij}^- = \frac{S_{j+1}^* - S_j}{S_j - S_i}. \tag{7.4}$$

We can now apply Davis' formulation (2.18)–(2.19) by introducing the forward/backward artificial viscosity coefficients

$$\begin{aligned} k_{ij}^+ &= \tfrac{1}{2} |v| \, (1 - |v|)[1 - \phi(r_{ij}^+)] \\ k_{ij}^- &= \tfrac{1}{2} |v| \, (1 - |v|)[1 - \phi(r_{ij}^-)] \end{aligned} \tag{7.5}$$

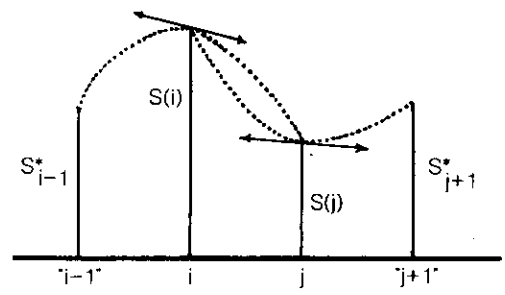

FIG. 6. Fictitious values at the fictitious nodes.

with $\phi(r) = \min(2r, 1)$, whence, according to (2.20), we deduce the effective artificial viscosity limiter to be used in (7.1c),

$$k_{ij} = k_{ij}(r_{ij}^+, r_{ij}^-) = \max(k_{ij}^+, k_{ij}^-). \tag{7.6}$$

To obtain an idea of the amount of viscosity introduced by the last term of the corrector equation (7.1c), we have first set $k_{ij} \equiv 1$ for all i, j, thus obtaining the highest possible level of viscosity; the results obtained for the test case of Sod's shock tube problem [50] are presented in Fig. 7.

On the other hand, when the limiters k_{ij} are defined as in (7.6) by Davis' formula, we obtained a substantial improvement in the accuracy (see Fig. 8, where the shock is sharp (3 points) and the contact discontinuity is captured in approximately 7 points); nevertheless we do not consider the resolution to be satisfactory. The same scheme has been applied to solve the problem of an unsteady flow in a channel with a cylindrical bump [44].

For the numerical calculations presented in Fig. 9, we find that full convergence has not been attained, thus leading to entropy lines which do not follow the streamlines

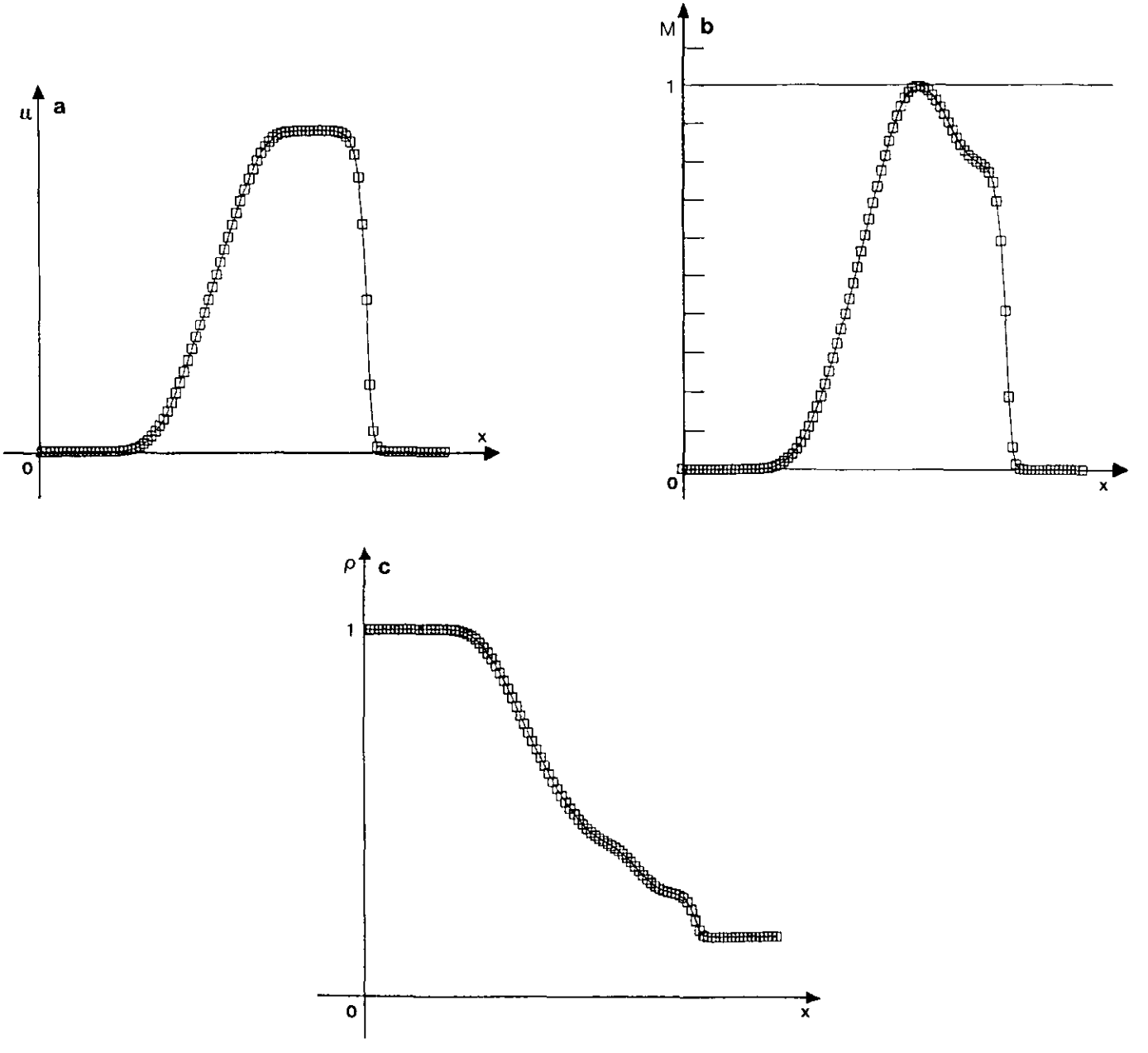

FIG. 7. Shock tube for the first-order version.

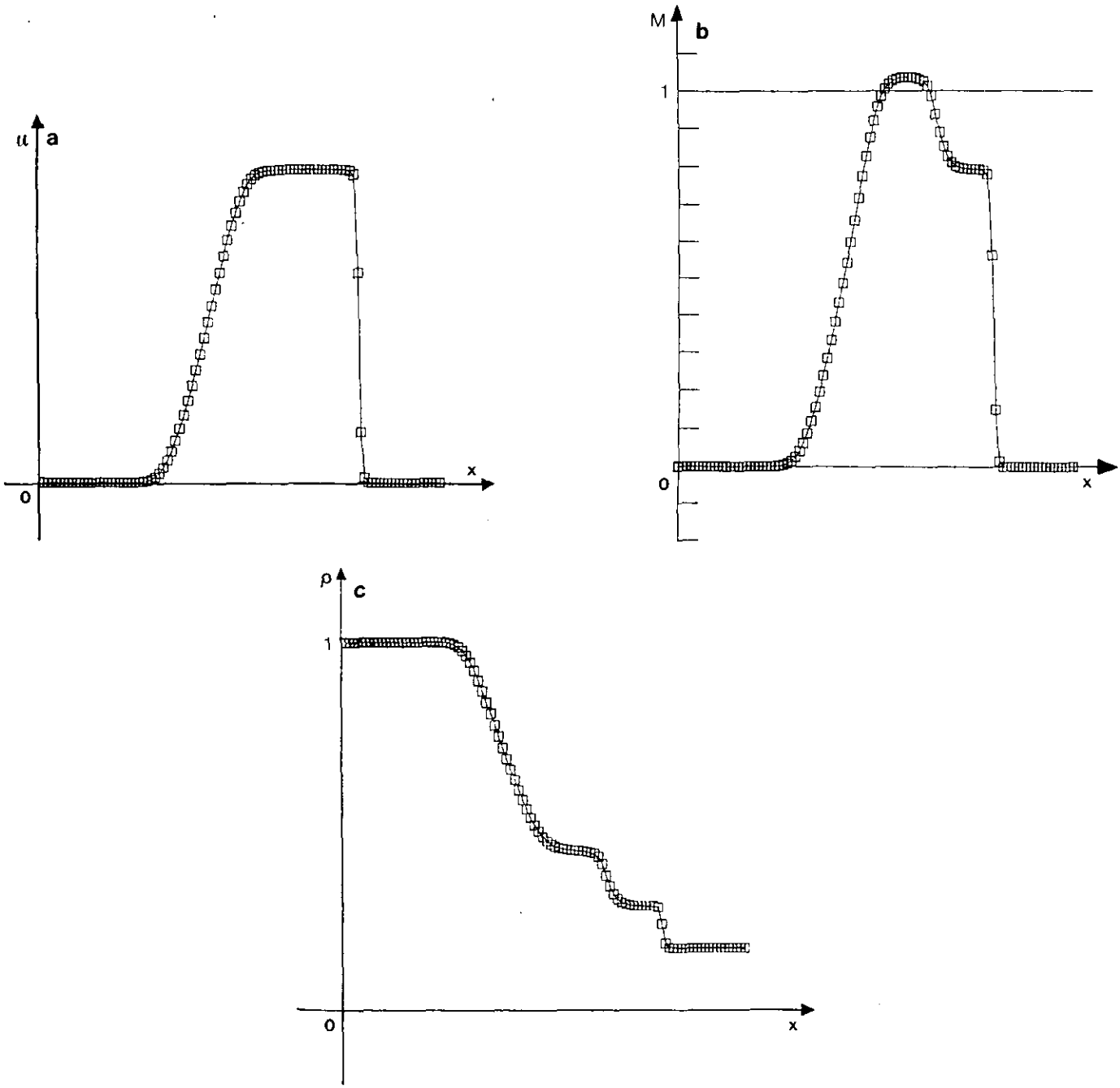

FIG. 8. Shock tube for the TVD version.

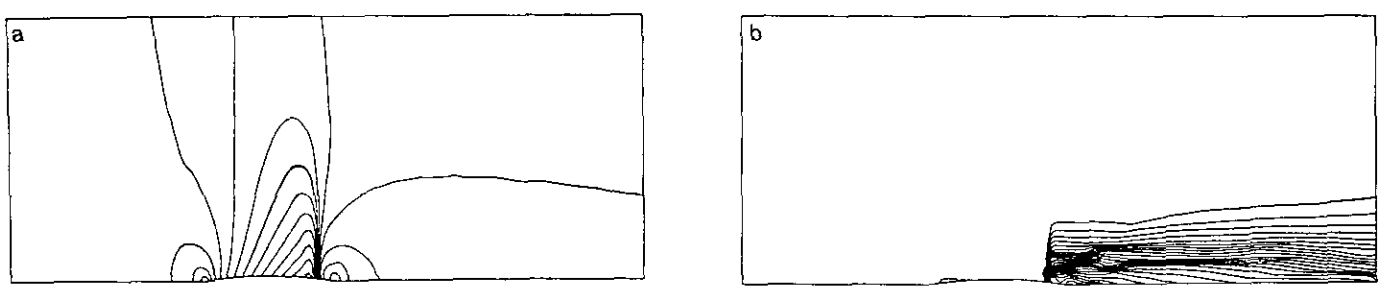

FIG. 9. Transonic channel flow; Richtmyer–Galerkin scheme with TVD-controlled viscosity.

closely enough. The shock, nevertheless, remains sharp, although the isomach lines appear to be fairly rounded in the upper part of the shock.

7.2. *Richtmyer–Galerkin/Osher Upwind Hybrid Scheme*

The Richtmyer–Galerkin scheme with symmetric TVD-controlled artificial viscosity presented in Section 7.1 has two major drawbacks:

(i) We have no guarantee that the combination of the segmentwise viscosity generated in 7.1 and the Lax–Wendroff second-order terms will ensure positivity.

(ii) The artificial viscosity introduced by (7.1)–(7.6) may be much too large, owing to the fact that, being a scalar viscosity, it does not take into account the velocities of the waves associated with the flow.

Moreover, it is of Lax–Friedrichs type and, therefore, only conditionally consistent.

We shall resort to Osher's approximate Riemann solver, which will appear within a barycentric combination of the (symmetric, second-order accurate) Richtmyer–Galerkin scheme and Osher's first-order flux decomposition upwind scheme.

In this hybrid scheme, the Lax–Wendroff term will completely disappear when the scheme switches to Osher's upwind scheme. We observe here that the symmetric terms included in Osher's formulation, of the form $[H(U_i)+H(U_j)]/2$, differ from those included in the Richtmyer–Galerkin scheme, which have the form $H((U_i+U_j)/2)$ and are more stable in a nonlinear context.

The proposed Richtmyer–Galerkin/Osher upwind hybrid scheme can be written with the same predictor step (7.1a) as in our first scheme (7.1), and the following:

Corrector step.

$$\begin{aligned}\text{area}(\text{cell}_i)(U_i^{n+1}-U_i^n) &= -\Delta t\Bigg\{\sum_{j\ \text{neighbour of}\ i}(1-k_{ij})\\ &\times\Bigg[\int_{GI}(F(U^P)|_T n_x+G(U^P)|_T n_y)\,d\sigma\\ &+\int_{IG'}(F(U^P)|_{T'} n_x+G(U^P)|_{T'} n_y)\,d\sigma\Bigg]\\ &+k_{ij}\Phi^{\text{Osher}}(U_i,U_j,\boldsymbol{\eta}_{ij})\Bigg\},\end{aligned}\tag{7.7a}$$

where

$$\boldsymbol{\eta}_{ij}=\int_{\partial\,\text{cell}_i\cap\partial\,\text{cell}_j}\mathbf{n}\,d\sigma\tag{7.7b}$$

and Φ^{Osher} is the numerical flux (4.21) corresponding to Osher's upwind flux splitting scheme (see, e.g., [38, 39] and k_{ij} is the artificial viscosity coefficient defined in Section 7.1.

For this second scheme, too, we found it interesting to compare the first-order version obtained by choosing $k_{ij}\equiv 1$ (i.e., Osher's first-order upwind scheme) with the hybrid version (7.7). This comparison was first performed for the

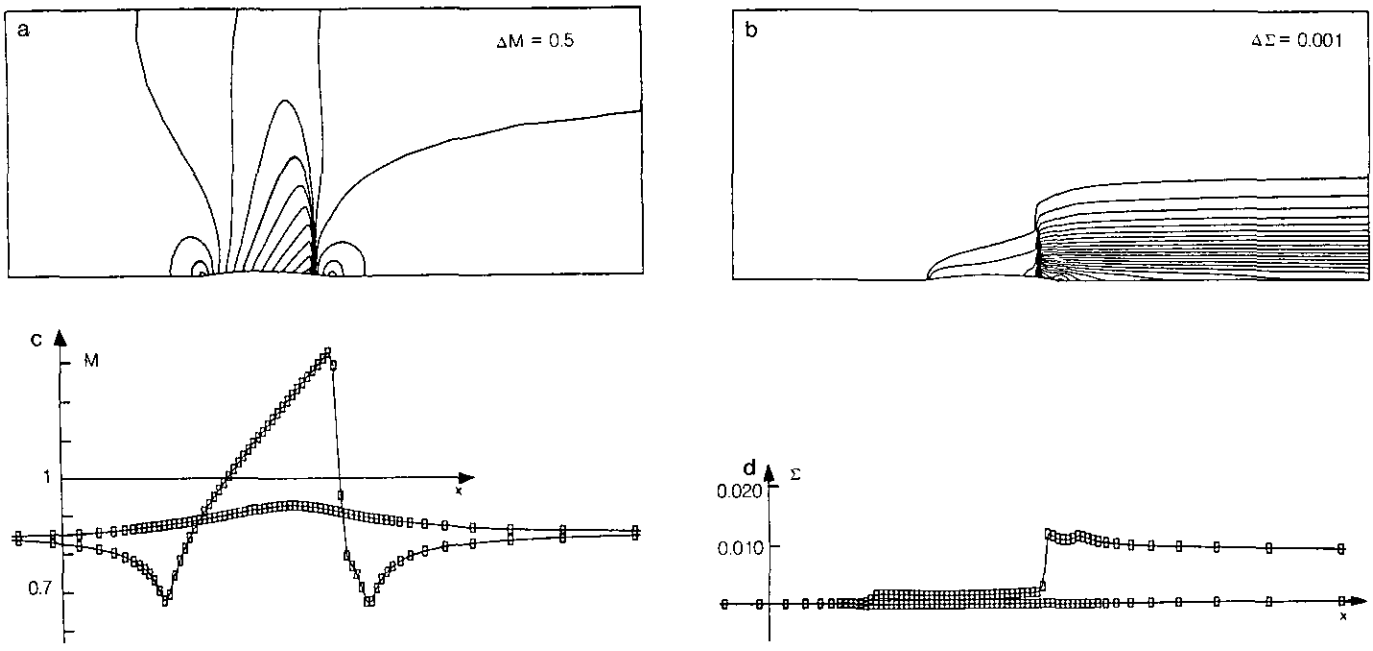

FIG. 10. Transonic channel flow; first-order upwind scheme.

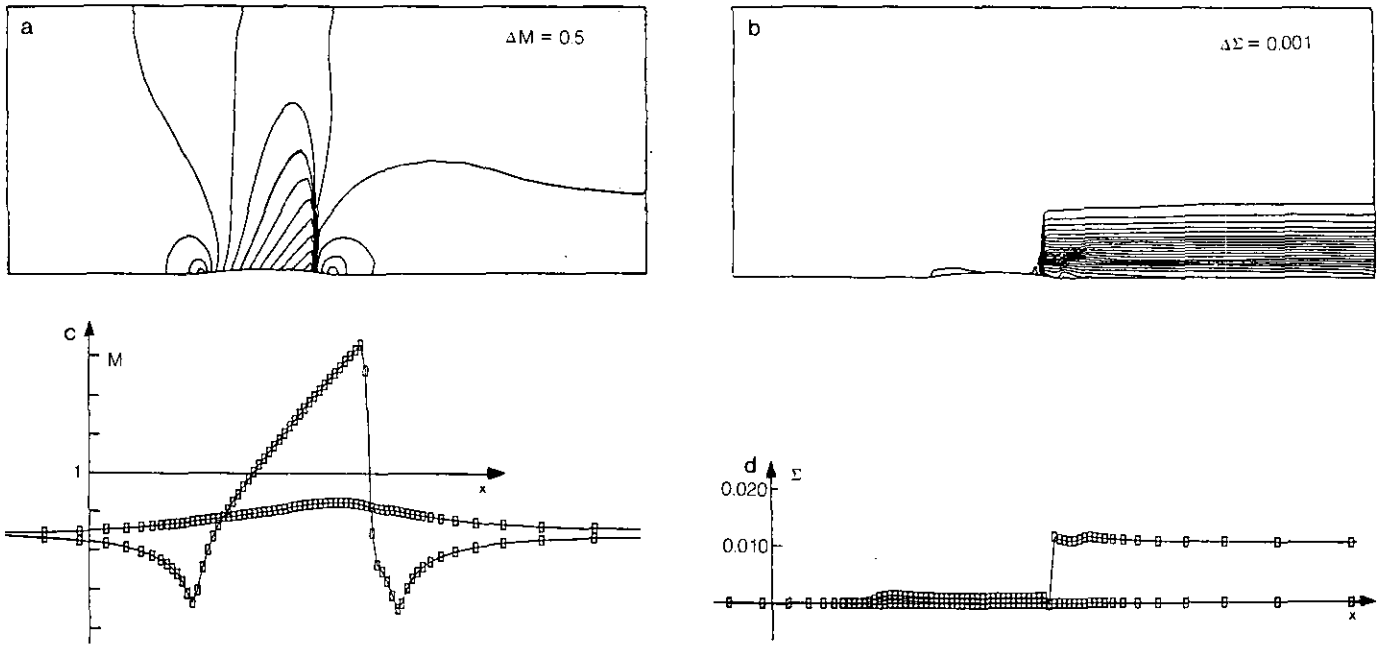

FIG. 11. Transonic channel flow; Richtmyer–Galerkin/Osher hybrid TVD scheme.

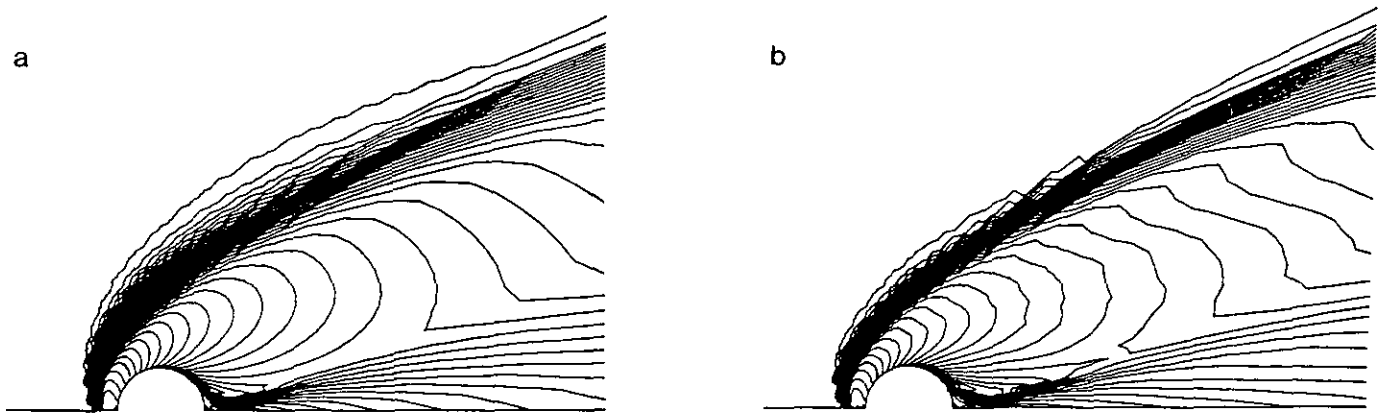

FIG. 12. Flow around a cylinder (Mach = 8.0); isomach contours for the above first-order and second-order TVD versions.

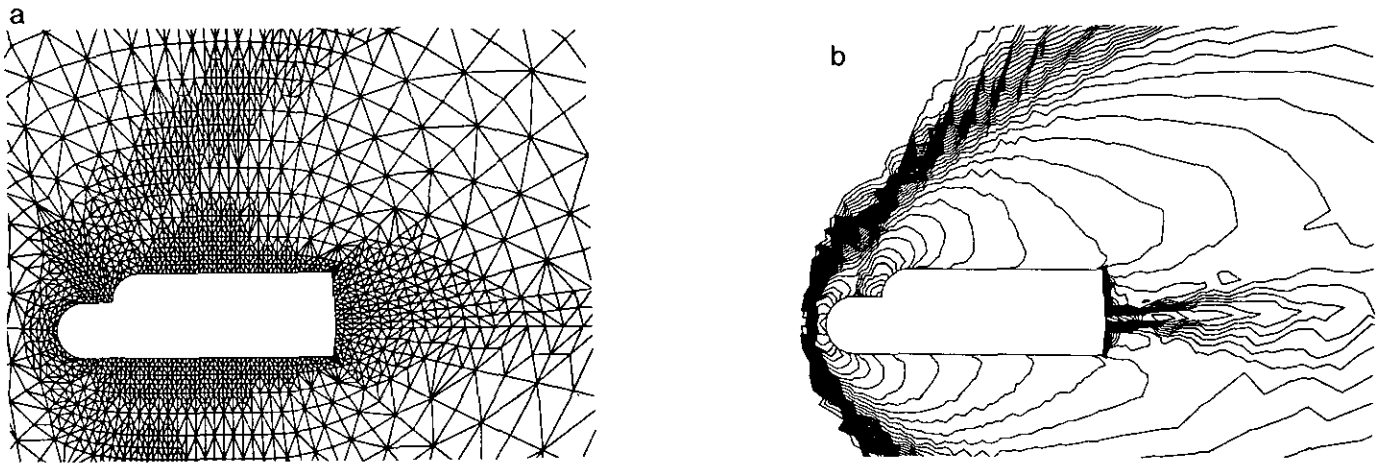

FIG. 13. Flow around a "space van" (Mach = 8.0); mesh and isomach contours, TVD scheme.

test problem of an unsteady flow through a channel with a cylindrical bump mentioned in Section 7.1. For this problem the first-order scheme already gives fairly good results (Fig. 10), and the only significant improvement brought by the second-order scheme concerns the isoentropic lines (Fig. 11).

In the second test case of a supersonic flow past a cylinder at $M_\infty = 8$, we obtain better evidence of the higher accuracy of the quasi-second-order hybrid scheme for the capture of the shock (Fig. 12).

A less academic test case is a flow around a "space van," for which we present, *for illustration of a non-structured triangulation*, a (partial) view of the mesh and Mach contours for a farfield Mach number of 8; the mesh was destructured by local refinement and is still rather coarse; the TVD version is applied and produces a rather stable result (Fig. 13).

7.3. *Central Difference (Symmetric TVD) MUSCL-like Scheme*

The Richtmyer–Galerkin/Osher upwind hybrid scheme is still affected with a rather annoying drawback: it uses a scalar viscosity limiter k_{ij} computed from a single scalar sensor, the Mach number. This may lead to global first-order accuracy for the numerical integration of all dependent variables, along each nodal segment which is more or less aligned with the local isomach lines.

One way to eliminate this difficulty consists in abandoning the notion of (viscous) flux limiter, resorting instead to

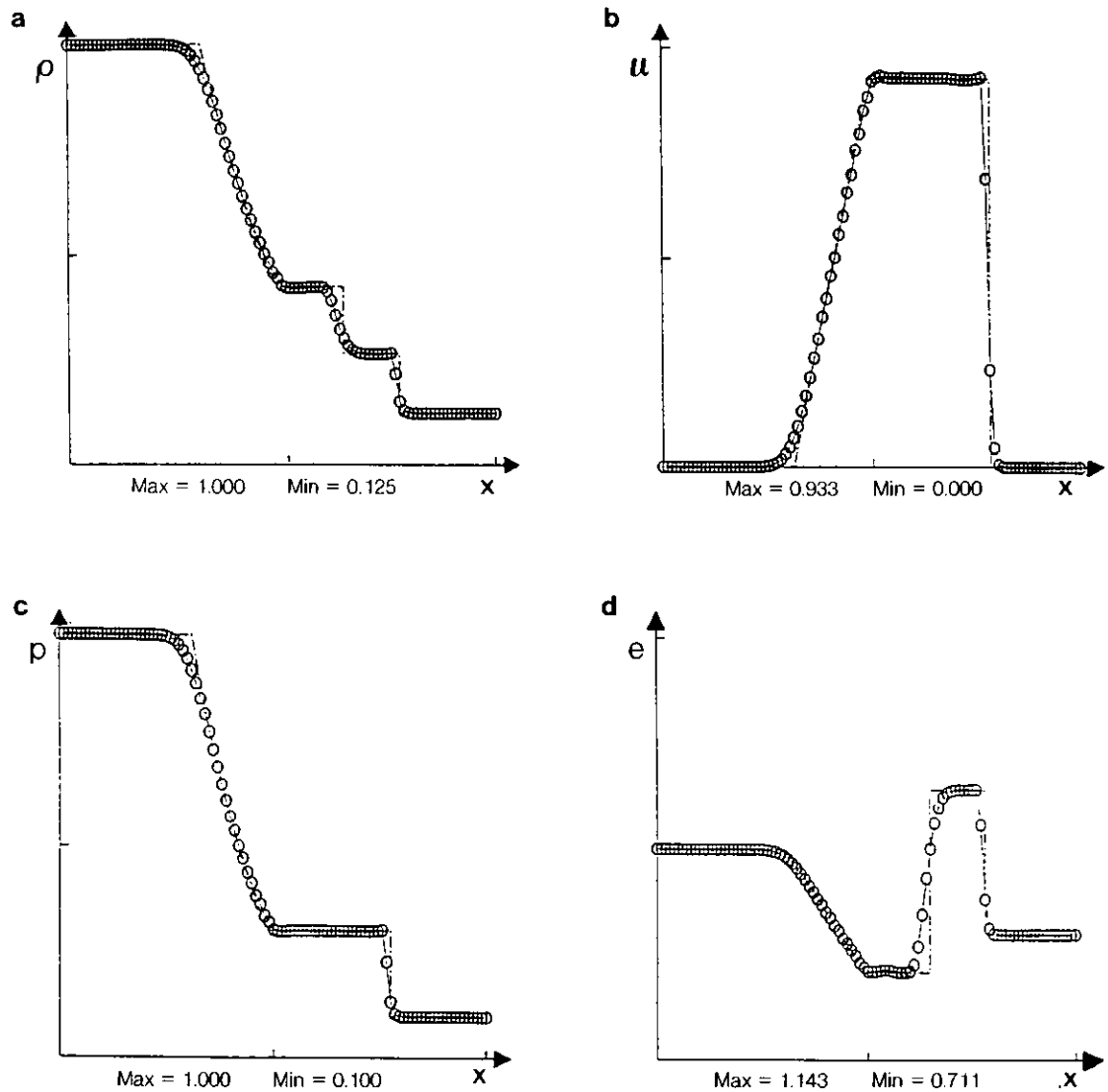

FIG. 14. Shock tube test for the central-MUSCL scheme.

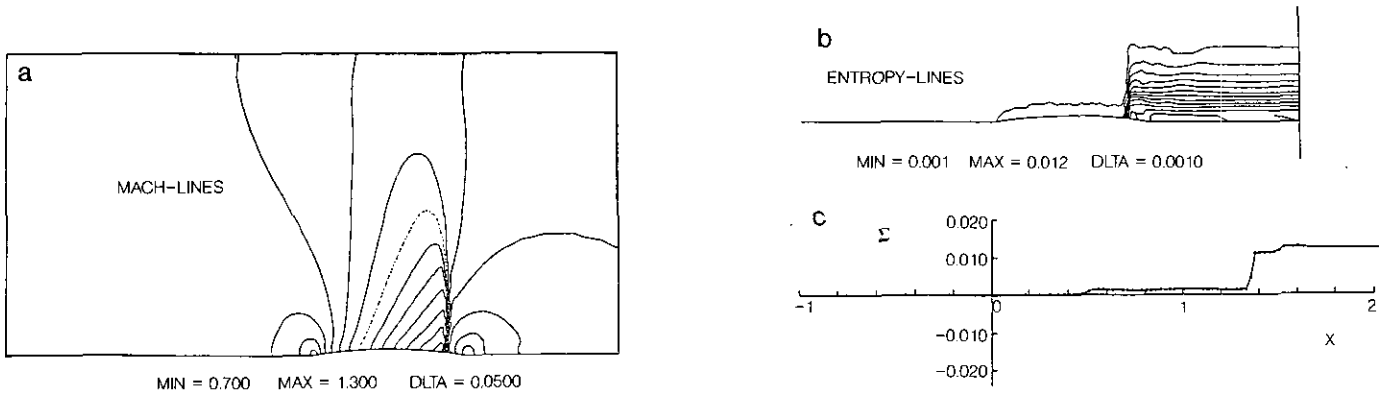

FIG. 15. Transonic channel flow test for the central-MUSCL scheme.

van Leer's MUSCL methodology in order to obtain a more sensitive type of artificial viscosity.

Other possibilities have been explored, among others, by Yee [69], and in a finite element context by Selmin [65].

The new scheme can be interpreted as a hybrid between a central scheme similar to the finite volume Galerkin method and an upwind first-order scheme. Using the semi-discretized notation, we shall write the proposed scheme as

$$\text{area}(\text{cell}_i)\frac{\partial U}{\partial t}+\sum_{j\ \text{neighbour of}\ i}\Phi(U_{ij}^{\text{cen}},U_{ji}^{\text{cen}},\boldsymbol{\eta}_{ij})=0 \qquad (7.8)$$

where Φ is Osher's approximate Riemann solver (4.21) [39] and the interpolated values U_{ij}^{cen}, U_{ji}^{cen} are defined with the help of the primitive variables $\tilde{U}=(\rho,u,v,p)$ as

$$\begin{aligned}\tilde{U}_{ij}^{\text{cen}}&=\frac{\tilde{U}_i+\tilde{U}_j}{2}+k_{ij}(\tilde{U})\frac{\tilde{U}_i-\tilde{U}_j}{2}\\ \tilde{U}_{ji}^{\text{cen}}&=\frac{\tilde{U}_i+\tilde{U}_j}{2}+k_{ij}(\tilde{U})\frac{\tilde{U}_j-\tilde{U}_i}{2},\end{aligned} \qquad (7.9)$$

where k_{ij} is defined from four conservative (partly fictitious) values of $\tilde{U}$,

$$k_{ij}=k_{ij}(\tilde{U}_{\text{"}i-1\text{"}},\tilde{U}_i,\tilde{U}_j,\tilde{U}_{\text{"}j+1\text{"}}) \qquad (7.10)$$

as described in Section 7.1, and $\tilde{U}_{ij}^{\text{cen}}=(\rho_{ij}^{\text{cen}},u_{ij}^{\text{cen}},v_{ij}^{\text{cen}},p_{ij}^{\text{cen}})$ while $U_{ij}^{\text{cen}}=(\rho_{ij}^{\text{cen}},\rho_{ij}^{\text{cen}}u_{ij}^{\text{cen}},\rho_{ij}^{\text{cen}}v_{ij}^{\text{cen}},e_{ij}^{\text{cen}})$.

We observe that for $k_{ij}=0$ we obtain the same values,

$$\tilde{U}_{ij}^{\text{cen}}=\tilde{U}_{ji}^{\text{cen}}=\frac{\tilde{U}_i+\tilde{U}_j}{2},$$

thus obtaining the centered scheme since, due to its consistency, the Riemann solver (4.21) reduces to $H((U_i+U_j)/2)$.

We obtain a Galerkin-type method which is not quite equivalent to a finite volume Galerkin scheme, as we take H (average of values of U) instead of an average of the values of H.

If $k_{ij}\equiv 1$, we obtain $U_{ij}^{\text{cen}}=U_i$, $U_{ji}^{\text{cen}}=U_j$ which results in Osher's first-order scheme.

For the central difference MUSCL-like scheme, we have again treated the test case of the shock tube (Fig. 14) and of the flow through a channel with a bump; in this last case, the results (Fig. 15), although not quite as good as we might have hoped, compared to those of Sections 7.1, 7.2, are nevertheless very similar. In the case where $k_{ij}\equiv 1$, the scheme is the same as the corresponding first-order scheme of Section 7.2.

In another test case, we computed a supersonic flow ($M_\infty=8$) past a blunt body. On Fig. 16 showing the

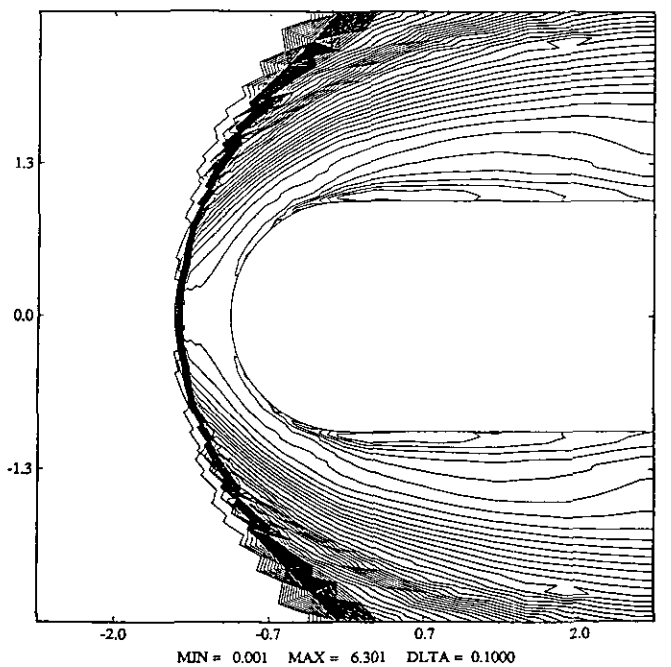

FIG. 16. Blunt body flow for the central-MUSCL scheme.

iso-entropic lines, we find that this scheme still contains a fair amount of viscosity, while allowing us to obtain much better results than with the first-order scheme.

8. CONCLUSION

Several methods for spatially stabilizing central differenced finite-element methods have been presented; they rely on TVD-like hybrid schemes between a first-order accurate version and a second-order one.

A special emphasis was put on the choice of the first-order accurate version (viscosity or upwinding), since it seems to be the main factor for obtaining an accurate hybrid scheme.

While the three presented schemes are easily applied to unsteady problems, convergence to steady state was difficult for each of them, due to the central-differenced component. Also the viscosity applied at stagnation points is too large and its reduction could be the subject of further research.

REFERENCES

1. F. Angrand, V. Boulard, A. Dervieux, J. Periaux, and G. Vijayasundaram, "Transonic Euler Simulation by Means of F.E.M. Explicit Schemes," 6th AIAA Computational Fluid Dynamics Conference, Danvers, MA, July 13–15, 1983; AIAA Paper 83-1924.
2. F. Angrand, A. Dervieux, L. Loth, and G. Vijayasundaram, Rapport INRIA No. 250 (Rocquencourt, 78153 Le Chesnay, France, 1983).
3. F. Angrand, and A. Dervieux, *Int. J. Numer. Methods Fluids* **4**, 749 (1984).
4. P. Arminjon, INRIA Report No. 520, April 1986; *SIAM Rev.*, to appear.
5. P. Arminjon, A. Dervieux, L. Fezoui, H. Steve, B. Stoufflet, in *Proceedings, 2nd Int. Conf. Hyperbolic Problems, Aachen, Germany, March 1988* edited by R. Jeltsch and J. Ballmann (Notes on Numer. Fluid Mechanics 24, Vieweg, Braunschweig, 1988).
6. P. Arminjon and A. Rousseau, *Comput. Methods Appl. Mech. Eng.* **49**, No. 1, 17 (1985).
7. P. Arminjon and L. Smith, *Comput. Methods Appl. Mech. Eng.* **100**, No. 2, 149 (1992).
8. K. Baba and M. Tabata, *RAIRO Numer. Anal.* **15**, 3 (1981).
9. J. P. Boris and D. L. Book, *J. Comput. Phys.* **11**, 38 (1973).
10. S. R. Chakravarthy and S. Osher, in *Proceedings, AIAA Comput. Fluid Dynamics Conference, Danvers, MA*, p. 363 (1983).
11. S. F. Davis, ICASE NASA Contractor Report 172373, Hampton, VA, June 1984.
12. J. A. Donea, *Int. J. Numer. Methods Eng.* **20**, 101 (1984).
13. J. A. Donea, L. Quartapelle, and V. Selmin, *J. Comput. Phys.* **70** (2), 463 (1987).
14. B. Engquist and S. Osher, *Math. Comput.* **34**, 45 (1980).
15. F. Fezoui, Rapport INRIA No. 358 (Rocquencourt, 78153 Le Chesnay, France, 1985).
16. J. E. Fromm, *J. Comput. Phys.* 3, 176 (1968).
17. J. L. Fromm, "A Numerical Study of Buoyancy Driven Flows in Room Enclosures," in *Lecture Notes in Physics*, Vol. 8 (Springer-Verlag, Berlin, 1971), p. 120.
18. S. K. Godunov, *Math. Sb.* **47**, 271 (1959). [Russian].
19. J. B. Goodman and R. J. Leveque, ICASE NASA Contractor Report 172484, Hampton, VA, October 1984.
20. G. D. van Albada, B. Van Leer, and W. W. Roberts, Jr., *J. Astron. Astrophys.* **108**, 76 (1982).
21. A. Harten, *J. Comput. Phys.* **49**, 357 (1983).
22. A. Harten, P. D. Lax, and B. van Leer, *SIAM Rev.* **25**, 35 (1983).
23. T. Ikeda, "Maximum Principle in Finite Element Models for Convection-Diffusion Phenomena," in *Lecture Notes Numer. Appl. Anal.*, Vol. 4 (North Holland/Kinokuniya, Amsterdam/Tokyo, 1983).
24. A. Jameson, "Numerical Solution of the Euler Equations for Compressible Inviscid Fluids," in *Numerical Methods for the Euler Equation of Fluid Dynamics*, edited by F. Angrand *et al.* (SIAM, Philadelphia, 1985).
25. P. D. Lax, *Hyperbolic Systems of Conservation Laws and the Mathematical Theory of Shock Waves*, CBMS Regional Conference Series in Appl. Math., Vol. 11 (SIAM, Philadelphia, 1973).
26. P. D. Lax and B. Wendroff, *Commun. Pure Appl. Math.* **13**, 217 (1960).
27. B. van Leer, *J. Comput. Phys.* **14**, 361 (1974).
28. B. van Leer, *J. Comput. Phys.* **23**, 276 (1977).
29. B. van Leer, *J. Comput. Phys.* **32**, 101 (1979).
30. B. van Leer, "Computational Methods for Ideal Compressible Flow," in *Comput. Fluid Dynamics*, von Karman Institute for Fluid Dynamics, Lecture Series 1983-04, (Hemisphere, Washington, DC, 1983).
31. A. Lerat and R. Peyret, *C. R. Acad. Sci. Paris Sér. A* **277**, 363 (1973).
32. A. Lerat and J. Sides, Proceedings, of the Conf. on Numer. Methods in Aeronautical Fluid Dynamics, University of Reading, March 29–April 1st, 1981.
33. R. Loehner, K. Morgan, J. Peraire, and M. Vahdati, NASA Contr. Rep. No. 178233, ICASE Rep, No. 87-4 (ICASE, Hampton, VA, 1987).
34. A. Majda and S. Osher, *Commun. Pure Appl. Math.* **32**, 797 (1979).
35. J. von Neumann and R. D. Richtmyer, *J. Appl. Phys.* **21**, 232 (1950).
36. S. Osher, *SIAM J. Numer. Anal.* **21**, 217 (1984).
37. S. Osher, *SIAM J. Numer. Anal.* **22** (5), 947 (1985).
38. S. Osher and S. Chakravarthy, *J. Comput. Phys.* **50** (3) 447 (1983).
39. S. Osher and S. Chakravarthy, *SIAM J. Numer. Anal.* **21**, 955 (1984).
40. S. Osher and F. Solomon, *Math. Comput.* **38**, 339 (1982).
41. A. K. Parrot and M. A. Christie, "FCT applied to the 2-D Finite Element Solution of Tracer Transport by Single Phase Flow in a Porous Medium," in *Proceedings, of the ICFD - Conf., on Num. Meth. for Fluid Dynamics II*, Reading, April 1985, edited by K. W. Morton and M. J. Baines (Academic Press, New York/London, 1986).
42. R. Peyret and T. D. Taylor, *Computational Methods for Fluid Flow* (Springer-Verlag, New York/Heidelberg/Berlin, 1983).
43. R. D. Richtmyer and K. W. Morton, *Difference Methods for Initial Value Problems* (Wiley, New York, 1967).
44. A. Rizzi and H. Viviand (Ed.) *Numerical Methods for the Computation of Inviscid Transonic Flows with Shock Waves*, Notes on Numerical Fluid Dynamics, Vol. 3 (Vieweg, Braunschweig/Wiesbaden, 1981).
45. P. L. Roe, in *Proceedings, 7th Inter. Conf. Num. Meth. Fluid Dynamics, Stanford/NASA Ames*, edited by W. G. Reynolds and R. Mac Cormack, Lecture Notes in Physics, No. 141 (Springer-Verlag, New York, 1981), p. 354.
46. P. L. Roe, *J. Comput. Phys.* **43**, 357 (1981).
47. P. L. Roe, ICASE Report No. 84-53, Hampton, VA, October 1984.
48. W. Schmidt and A. Jameson, "Euler Solvers as an Analysis Tool for

Aircraft Aerodynamics," in *Recent Advances in Numerical Methods in Fluids*, Vol. 4, edited by W. G. Habashi (Pineridge Press, Swansea, UK, 1983).

49. J. Smoller, *Shock Waves and the Reaction-Diffusion Equations* (Springer-Verlag, Berlin/Heidelberg/New York, 1983).
50. G. A. Sod, *J. Comput. Phys.* **27**, 1 (1978).
51. J. Steger and R. F. Warming, *J. Comput. Phys.* **40**, 263 (1981).
52. P. K. Sweby, *SIAM J. Numer. Anal.* **21**, 995 (1984).
53. M. Tabata, *Mem. Numer. Math.* **4**, 47 (1977).
54. T. Ushijima, *Mem. Numer. Math.* **6**, 65 (1979).
55. G. Vijayasundaram, Thesis, University of Paris VI, 1983 (unpublished).
56. G. Vijayasundaram, in *Proceedings, Workshop on Numer. Methods for the Euler Equations for compressible inviscid fluids, INRIA, Versailles-Rocquencourt, Dec. 1983*, edited by Angrand *et al.* (*SIAM, Philadelphia*, 1986).
57. G. Vijayasundaram, *J. Comput. Phys.* **63**, 416 (1986).
58. H. C. Yee, R. F. Warming, and A. Harten, in *Proceedings, AIAA Comp. Fluid Dynamics Conference, Danvers, MA*, pp. 110–127.
59. P. R. Woodward and P. Colella, *J. Comput. Phys.* **54**, 174 (1984).
60. A. Jameson, MAE Report No. 1653, Princeton University, March 1984 (unpublished).
61. P. Arminjon and A. Dervieux, INRIA Report No. 1111, October 1989 (Rocquencourt, 78153 Le Chesnay, France, 1989).
62. R. Courant, E. Isaacson, and M. Rees, *Commun. Pure Appl. Math.* **5**, 243 (1952).
63. R. MacCormack, AIAA paper No. 69-354
64. D. L. Book, J. P. Boris, and K. Hain, *J. Comput. Phys.* **18**, 248 (1975).
65. V. Selmin, INRIA Reports No. 706 and 708 (Rocquencourt, 78153 Le Chesnay, France, 1987).
66. B. van Leer, *J. Comput. Phys.* **23**, 263 (1977).
67. A. Harten, J. MacHyman, and P. Lax, *Commun. Pure Appl. Math.* **29**, 296 (1976).
68. A. Harten, *Math. Comput.* **32**, 363 (1978).
69. H. C. Yee, *J. Comput. Phys.* **57**, 327 (1987).
70. A. Jameson, *Lectures Appl. Math.* **22**, 345 (1985).
71. A. Harten, *SIAM J. Numer. Anal.* **21**, 1–23 (1984).